

**NIST Grant/Contractor Report  
NIST GCR 18-049**

# **Fuse 47 Apartment Complex Fire Modeling Analysis**

This publication is available free of charge from:  
<https://doi.org/10.6028/NIST.GCR.18-049>

**NIST Grant/Contractor Report  
NIST GCR 18-049**

**Fuse 47 Apartment Complex Fire  
Modeling Analysis**

This publication is available free of charge from:  
<https://doi.org/10.6028/NIST.GCR.18-049>

December 2018



U.S. Department of Commerce  
*Wilbur L. Ross, Jr., Secretary*

National Institute of Standards and Technology  
*Walter Copan, NIST Director and Undersecretary of Commerce for Standards and Technology*

## **Disclaimer**

Certain commercial entities, equipment, or materials may be identified in this document in order to describe an experimental procedure or concept adequately. Such identification is not intended to imply recommendation or endorsement by the National Institute of Standards and Technology, nor is it intended to imply that the entities, materials, or equipment are necessarily the best available for the purpose.

## **Copyright, Use, and Licensing**

This NIST Grant/Contractor Report was prepared for NIST under the indefinite delivery/indefinite quantity (IDIQ) contract SB1341-12-CQ-0014 for Support Services for the NIST Disaster Failure Studies Program. Those portions of the studies prepared for NIST under contract may be subject to US or foreign Copyright held by the contractor. While NIST retains the right to distribute copies to the public in any manner and for any purpose, and to have or permit others to do so on NIST's behalf, distribution or use of the work by others may require that permissions or licenses first be obtained from the contractor.

In accordance with Public Law 100-519, Section 107 (Oct 24, 1988), NIST maintains a research information center to support the research, publishing, and preservation needs required to fulfill the scientific and technical mission of NIST. This includes publishing the NIST Technical Series: technical reports and Journal of Research of NIST. Works authored by NIST employees are not subject to Copyright protection within the United States; foreign rights are reserved. To the extent NIST may assert rights outside of the United States, the public is granted the non-exclusive, perpetual, paid-up, royalty-free, worldwide right to reprint works in all formats including print, electronically, and online, and in all subsequent editions, and derivative works. Please use the recommended citation format below followed by "Republished courtesy of the National Institute of Standards and Technology." Some works published by NIST may have been written by third parties and may be subject to copyright protection.

## **How to Cite this NIST Technical Series Publication**

Jensen Hughes (2018) Fuse 47 Apartment Complex Fire Modeling Analysis. National Institute of Standards and Technology, Gaithersburg, MD, NIST GCR 18-049. <https://doi.org/10.6028/NIST.GCR.18-049>



# JENSEN HUGHES

3610 Commerce Drive | Suite 817  
Baltimore, MD 21227 USA  
jensenhughes.com  
+1 410-737-8677  
Fax: +1 410-737-8688

**NIST 17-04781**

**Disaster and Failure Studies Research  
Program Support Services**

**Fuse 47 Apartment Complex  
Fire Modeling Analysis**

**Submitted by:**

JENSEN HUGHES

**December 28, 2018**

Project #: 1STH17128.000

## TABLE OF CONTENTS

<b>1.</b>	<b>SCOPE OF WORK .....</b>	<b>1</b>
<b>2.</b>	<b>SYNOPSIS OF INCIDENT .....</b>	<b>2</b>
<b>3.</b>	<b>BUILDING DETAILS .....</b>	<b>2</b>
<b>4.</b>	<b>FIRE SPREAD .....</b>	<b>2</b>
	<b>4.1. Weather .....</b>	<b>2</b>
	<b>4.2. Observations .....</b>	<b>3</b>
	<b>4.3. Timeline.....</b>	<b>7</b>
<b>5.</b>	<b>METHODOLOGY.....</b>	<b>8</b>
	<b>5.1. High-Resolution Models .....</b>	<b>8</b>
	5.1.1. Ignition and Fire Spread from 6 <sup>th</sup> Floor to Attic Space.....	9
	5.1.2. Fire Spread through the Attic.....	11
	<b>5.2. Monte Carlo Simulations .....</b>	<b>14</b>
	<b>5.3. Low-Resolution Simulations.....</b>	<b>16</b>
	5.3.1. Baseline Model.....	16
	5.3.2. Baseline Model with Exterior Walls Removed .....	18
<b>6.</b>	<b>RESULTS .....</b>	<b>19</b>
	<b>6.1. Ignition and Spread from 6<sup>th</sup> Floor to Attic Space .....</b>	<b>19</b>
	<b>6.2. Monte Carlo Simulations .....</b>	<b>23</b>
	<b>6.3. High-Resolution Simulations .....</b>	<b>27</b>
	6.3.1. Baseline Model.....	27
	6.3.2. Baseline Model with Sprinklers .....	29
	6.3.3. Baseline Model with 3,000 sq. ft. Area Partitioned .....	30
	6.3.4. Baseline Model with 10,000 sq. ft. Area Partitioned .....	31
	<b>6.4. Low-Resolution Simulations.....</b>	<b>32</b>
	6.4.1. Baseline Simulation .....	32
	6.4.2. Baseline Model with 10,000 sq. ft. Area Partitioned .....	33
	6.4.3. Baseline Model with Sprinklers Active .....	34
	6.4.4. Baseline Model with Exterior Walls Removed .....	36
<b>7.</b>	<b>CONCLUSIONS.....</b>	<b>36</b>
<b>8.</b>	<b>REFERENCES.....</b>	<b>38</b>
	<b>APPENDIX A: FDS Input Files Delivered to NIST .....</b>	<b>40</b>

## 1. SCOPE OF WORK

The National Institute of Standards and Technology (NIST) has a long and impressive history of seeking to improve the safety of buildings, their occupants, and emergency responders through studies of building failures. Since 1969, NIST has investigated about 40 earthquakes, hurricanes, building and construction failures, tornadoes, and fires. These studies have resulted in major and far reaching changes to building and fire codes, standards, and practices. The study of disaster and failure events is essential for improving the performance of buildings and infrastructure, the safety of building occupants, and for evaluating the adequacy of codes, standards, practices, evacuation and emergency response procedures, and the current state-of-knowledge for structures. The results of disaster and failure studies help NIST develop community-scale loss estimation tools to predict consequences of disasters, leading to increased resilience.

Over the last four years, there have been a series of fires that have occurred in buildings under construction. Recent fires in buildings prior to being occupied include:

- Da Vinci Apartments – Los Angeles, CA; December 8, 2014  
Seven story, \$30M damage
- Metropolitan Apartments – Raleigh, NC; March 17, 2017  
Six story, \$12M damage
- City Place Apartments – Overland Park, KS; March 20, 2017  
Five story, \$20M damage, 22 other homes, \$5M damage
- Fuse 47 Apartments - College Park, MD; April 24, 2017  
Seven story, \$39M damage

Collectively, these fires demonstrate that most of the fire protection systems become effective only after occupancy, and are not effective during the construction phase. While individually, these fires may not rise to the level of requiring a detailed study and reconstruction, taken together, they highlight the need to better understand fire protection systems during the construction phase of buildings. One potential recommendation of a building construction fire study would be to incorporate fire protection systems during the construction phase.

To further advance the Disaster and Failure Studies Program, additional expertise and skills are needed. Specifically, expertise is needed to initialize the fire model input parameters and execute simulation runs using the Fire Dynamic Simulator (FDS) computer fire model. The Fuse 47 apartment building plans, dimensions, materials, and ventilation conditions need to be set-up for simulations to be run using FDS.

JENSEN HUGHES has input the building, floor, and room dimensions; materials of construction; ventilation openings; and fire protection systems components from construction design drawings into the Fire Dynamics Simulator. Initial fires(s) and subsequent fire automatic suppression activities have been incorporated into the model. JENSEN HUGHES has also exercised the model to simulate different fire spread and what-if scenarios according to the list of tasks provided as Table 1.

**Table 1. Descriptions of Tasks and Associated Deliverables**

<b>Task</b>	<b>Description</b>	<b>Deliverable</b>
1	Kick-off meeting	N/A
2	Construct a high-resolution grid case for the Fuse 47 apartment fire	PyroSim and Fire Dynamic Simulator Input Data File
3	Construct a low-resolution grid case for the Fuse 47 apartment fire	PyroSim and Fire Dynamic Simulator Input Data File
4	Run the high-resolution case to optimize for known fire spread timeline	Fire Dynamic Simulator Output Data File
5	Run the high-resolution case with sprinklers and fire barriers	Fire Dynamic Simulator Output Data File
6	Run the low-resolution case	Fire Dynamic Simulator Output Data File
7	Documentation	Report (Microsoft Word format)

## 2. SYNOPSIS OF INCIDENT

The Fuse 47 Apartment Complex fire occurred at approximately 9:30 am on Monday, 24 April 2017, in College Park, Maryland. Reports indicate that the fire was showing from the fifth and sixth floors, and was rapidly extended to the top floor and roof. Part of the roof on the eastern side of the structure collapsed, and the roads near the fire scene were closed for much of the day. The smoke from the fire forced the evacuation of 68 residents of a senior living facility across the street, and resulted in the temporary closure of the nearby University of Maryland. Fire officials reported that the fire was particularly difficult to fight, as the back side of the complex was constructed into a hillside, and the adjacent building was under construction, preventing firefighter access on three sides. By 3:00 pm, it was reported that the fire was under control, with hot spots remaining. Firefighters were at the scene through Monday night and into Tuesday morning using ladder trucks to spray water on the upper section of the structure.

Construction workers were on site at the time of the fire, and all were safely evacuated. Initial media reports indicated that one firefighter, suffering fatigue, was transported to the hospital for evaluation, while an emergency management official suffered an injured ankle. A resident of the senior living facility across the street was sent to the hospital after experiencing breathing difficulty.

Initial damage was estimated to be over \$39 million. Fire officials indicated that, due to excessive damage to the upper floors, the interior of the structure had to be shored up before firefighters and investigators could gain entrance to the fire scene. The cause of the blaze has not been determined and is under investigation. Since the incident, the building has been demolished and rebuilt as the Alloy by Alta.

## 3. BUILDING DETAILS

The FUSE 47 apartment complex was a pedestal-type building with the first two levels containing a parking garage constructed of poured-concrete. Five additional stories of lightweight wood frame construction were built on top of the concrete pedestal, which was slated to contain retail stores and 250 apartments. At the time of the fire, the seven-story apartment complex was under construction, nearing completion, and scheduled for occupancy in the summer of 2017. Since the building complex was still under construction, it reportedly had no active fire protection systems in service.

## 4. FIRE SPREAD

### 4.1. Weather

Weather data collected over the course of April 24, 2017 at College Park Airport, approximately 1 mile SSE of the FUSE 47 building, is presented in Table 2. Over the course of the fire, the wind was generally approximately 8 mph from the northeast and the air temperature increased from approximately 51°F at 9:21 AM to 56°F at 1:21 PM and decreased to approximately 52°F at 4:01 PM.

**Table 2. Weather data collected at College Park Station on April 24, 2017 [1]**

Time	Temperature	Wind	Wind Speed	Condition
9:21 AM	51°F	NE	5 mph	Cloudy
9:41 AM	50°F	NE	8 mph	Cloudy
10:01 AM	50°F	NNE	6 mph	Cloudy
10:21 AM	51°F	NE	5 mph	Cloudy
11:21 AM	53°F	ENE	6 mph	Cloudy
12:01 PM	55°F	ENE	6 mph	Cloudy
12:21 PM	55°F	NNE	8 mph	Cloudy
12:41 PM	56°F	NE	7 mph	Cloudy
1:01 PM	56°F	NE	8 mph	Cloudy
1:21 PM	56°F	NE	6 mph	Cloudy
1:41 PM	56°F	ENE	7 mph	Cloudy
2:01 PM	53°F	ENE	5 mph	Cloudy
2:21 PM	52°F	NE	6 mph	Cloudy
2:41 PM	52°F	NNE	5 mph	Cloudy
3:01 PM	52°F	NNE	6 mph	Cloudy
3:21 PM	52°F	NNE	3 mph	Cloudy
3:41 PM	52°F	NNE	6 mph	Cloudy
4:01 PM	52°F	ENE	5 mph	Cloudy

#### 4.2. Observations

All references made in this section were provided to JENSEN HUGHES by NIST personnel and are named identical to the file names provided by NIST. The fire department was notified of a fire on the sixth floor of the FUSE47 building shortly after 9:30 AM on April 24, 2017. An image of the development of the fire taken at 9:37 AM on April 24 [MobilePhoto\_DayOfFire] is provided as Figure 1. The image shows that flames were extending out of the 6<sup>th</sup> floor apartment where the fire originated prior to arrival of the fire department.



**Figure 1. Photograph showing flames extending out of 6<sup>th</sup> floor apartment taken at 9:37 AM on April 24, 2017 [MobilePhoto\_DayOfFire]**

The first fire engine arrived at the scene at approximately 9:40 AM [E122 Arrival (V1)]. Several firefighters recorded the suppression efforts using GoPro cameras attached to their helmets. A still image from one of these recordings estimated to be from approximately 9:41 AM that is provided as Figure 2 shows further development of the flames in the 6<sup>th</sup> floor apartment with the construction doors to the exterior of the 6<sup>th</sup> floor apartment severely damaged [2:09 SID Helmet Cam]. Flames can also be seen extending out of the south facing window on the south east of the 6<sup>th</sup> floor apartment and the east facing window opening. A still image from approximately 9:44 AM is provided as Figure 3 and shows apparent ignition along the edge of the construction doors on the exterior of the 7<sup>th</sup> floor apartment [5:35 SID Helmet Cam].



**Figure 2. Still image from approximately 9:41 AM showing severe damage to construction doors on exterior of 6th floor apartment and flames extending out of the southeastern and eastern windows from the 6th floor apartment [2:09 SID Helmet Cam].**



**Figure 3. Still image from approximately 9:44 AM showing flames extending out of the southeastern and eastern windows from the 6th floor apartment [5:35 SID Helmet Cam].**

Records indicated that water was applied to the 6<sup>th</sup> floor apartment fire from a deck gun on a fire engine starting at approximately 9:44:45 AM [5:50 SID Helmet Cam]. Video and photographs from the scene appear to show that the fire spread to the bedroom west of the original fire room after application of water. Figure 4 shows flames extending out of the window openings in the 6<sup>th</sup> floor southern bedroom at approximately 9:48 AM [8:53 SID Helmet Cam]. It is also evident that the wooden exterior of the building in the vicinity of the 6<sup>th</sup> floor bedroom window openings had also ignited at this time. Flames in the southeast of the original fire room are visible in Figure 5, which shows a still image from approximately 9:49 AM [10:11 SID Helmet Cam].



**Figure 4. Still image from approximately 9:48 AM showing flames extending out of the 6<sup>th</sup> floor apartment bedroom window openings [8:53 SID Helmet Cam].**



**Figure 5. Still image from approximately 9:49 AM showing flames extending out of the 6<sup>th</sup> floor apartment bedroom window openings with apparent re-ignition in the original fire room [10:11 SID Helmet Cam].**

At 9:50 AM, firefighter attack from the interior of the apartment building appeared to extinguish much of the fire that was present on the 6<sup>th</sup> floor. Figure 6 shows the smoke and steam pouring from the 6<sup>th</sup> floor immediately after application of water from the interior of the building [12:17 SID Helmet Cam]. There was a report of visible flames in the ceiling of the 7<sup>th</sup> floor living room accompanied by heavy smoke in the 7<sup>th</sup> floor at approximately 10:01 AM [22:31 SID Helmet Cam]. Firefighters began performing suppression operations from the 7<sup>th</sup> floor apartment affected by the fire at approximately 10:01 AM that included tearing down the ceiling as well as insulation in the attic space and applying water to the flames in the attic.



**Figure 6. Still Image from approximately 9:51 AM showing the immediate result of application of water to the 6<sup>th</sup> floor from the interior of the building [12:17 SID Helmet Cam].**

The fire in the attic space propagated through the attic apparently igniting prefabricated trusses and combustible sheathing in the roofing assembly. The still image captured at approximately 10:03 AM shown in Figure 7 shows flames visible on the roof in close proximity to the opening in the 7<sup>th</sup> floor living room ceiling [12:00 Firefighterhelmetcamoutdoors1]. During this time, firefighters in other areas of the 7<sup>th</sup> floor continued conducting suppression activities by tearing down the ceiling and applying water to the fire spreading through the attic space.



**Figure 7. Still image from approximately 10:03 AM showing flames present at the roof level directly above the original fire room location [12:00 Firefighterhelmetcamoutdoors1].**

A still image from approximately 10:18 AM presented as Figure 8 shows significant smoke development in the attic space and venting of the smoke in the attic space apparently via the roof ventilators [4:00 We Need 10ft Hooks (V5)]. It is evident that all flames in the 6<sup>th</sup> and 7<sup>th</sup> floor apartments that were affected by the fire had been extinguished prior to 10:18 AM. In the range of approximately 10:31 to 10:33 AM, flames were visible at the roof level of the apartment building [8:30 Side Alpha Footage (V6)] [2:20 Side Alpha Footage (2) (V7)]. The location of the flames in Figure 9 appear to indicate that these flames may be extending from the passive roof ventilator.



**Figure 8. Smoke venting from the roof-level passive ventilators at approximately 10:18 AM [4:00 We Need 10ft Hooks (V5)]**



**Figure 9. Flames extending from the roof level at approximately 10:33 AM [2:20 Side Alpha Footage (2) (V7)]**

Concurrent with firefighting operations on the 7<sup>th</sup> floor were suppression efforts on the roof of the building. Helmet camera footage from 11:50 AM show suppression efforts on the roof already underway [0:14 Trench Ops]. These efforts included attacking the open flames visible on the roof with fire hoses and cutting a trench into the roof to directly apply water to the open flames in the attic space. Flames were

visible at the roof level on the western edge of the northwest corner of the eastern wing of the building at approximately 11:50 AM (Figure 10) [0:14 Trench Ops] and grew significantly by approximately 12:05 PM (Figure 11) [

14:30 Trench Ops].



**Figure 10. View from the roof of the western wing of the building at 11:50 AM [0:14 Trench Ops]**



**Figure 11. View from the western wing of the building looking east at approximately 12:05 PM [14:30 Trench Ops]**

Flames were visible in the attic space at the trench cut into the roof at approximately 12:16 PM [11:16 Trench Ops 2] and was persistent in still images taken from video at 1:16 PM [10:45 Trench Ops 6]. Firefighting efforts continued from the 7<sup>th</sup> floor and the roof of the building and there was a report that local fires were still burning at approximately 4:00 PM.

#### **4.3. Timeline**

The major events from footage collected on the day of the fire that were used to compare to the simulation results are provided in

Table 3. The most important observations that formed the foundation for validation of the set of properties for validation of the Monte Carlo simulation and fire spread through the attic space were the first observation of flames in the attic at 10:01 AM and the observation of flames extending from the roof at 10:33 AM. The upper membrane of the roof assembly was defined as non-combustible, so the only possible point for penetration of the fire through the roof was at the passive ventilators. It was assumed that the flames observed at the roof at 10:33 AM extended from the southeastern-most ventilator. The datum against which the high-resolution attic fire spread simulation results were compared was approximately 30 minutes from the beginning of the attic spread simulation to the time when flames extended from the ventilator.

**Table 3. Timeline of major events observed in fire documentation**

Time	Event	Reference
~9:30 AM	Fire discovered in 6 <sup>th</sup> floor apartment	
9:37 AM	Flames extending from the construction doors on the 6 <sup>th</sup> floor	MobilePhoto_DayOfFire
9:41 AM	Construction doors have fallen from building. Flames extending from windows on south and east side of 6 <sup>th</sup> floor apartment	2:09 SID Helmet Cam
9:48 AM	Flames visible in bedroom of 6 <sup>th</sup> floor apartment	8:53 SID Helmet Cam
10:01 AM	Report of flames visible through 7 <sup>th</sup> floor in attic space	22:31 SID Helmet Cam
10:33 AM	Flames seen extending from roof	2:20 Side Alpha Footage (2) (V7)]
12:16 PM	Flames visible in attic at trench cut into roof at firewall	11:16 Trench Ops 2
4:00 PM	Report that local fires were still burning	

## 5. METHODOLOGY

FDS models were constructed to simulate the fire growth and flame spread during the FUSE47 incident as well as to conduct a parametric study on the effect of several passive and active fire protection elements on the overall fire growth from the baseline cases. A high-resolution model of the compartment of origin and the attic space was constructed and baseline simulations of the high-resolution model were validated against observations made during the incident. A low-resolution model that encompassed a larger portion of the building, the majority of which was not involved in the fire incident, was constructed to investigate the effect of the degree of completeness of wall and ceiling assemblies as well as sprinkler activation on large-scale fire growth throughout the building. The details of the various models are presented in the following sections.

### 5.1. High-Resolution Models

A high-resolution FDS model was constructed to simulate ignition and growth of the fire in the 6<sup>th</sup> floor apartment, spread of the fire to the 7<sup>th</sup> floor and attic space, and spread of the fire through the attic space. The intent of this model was to improve understanding of the fire dynamics phenomena that resulted in the fire development and flame spread that was observed and to validate the model against observations from the incident. An additional high-resolution model was constructed with sprinklers defined in the locations where they were installed in the attic space to investigate the effect these sprinklers would have had on the spread of the fire had the sprinklers been operational prior to completion of construction of the apartment building.

Several trial simulations were conducted to investigate possible methodologies for modeling the trusses and insulation in the attic space. The two methodologies used to describe the truss geometries resulted in a representation of the trusses as static Lagrangian particles and a representation of the trusses as obstructions that conformed to the rectilinear mesh. The two methodologies used to describe ignition and burning of the trusses included the simple pyrolysis model, which required definition of the ignition temperature and a heat release rate per unit area (HRRPUA), and the complex pyrolysis model which required definition of Arrhenius parameters, pyrolysis product yields, and heat of reaction for the modeled pyrolysis reaction.

A combination of these methodologies was used to simulate burning of the trusses and flame spread in the attic space with various configurations to determine the relative effect of each on the rate of fire spread. It was determined that the method of defining the trusses as collections of particles was too computationally expensive to yield a feasible solution and there was also the concern that particles defined in this way do not provide adequate resistance to fluid flow, which was expected to be a significant driving force in the fire spread through the attic space. All models and simulations presented in this work defined the trusses as rectilinear obstructions that conformed to the underlying mesh.

It was determined that the use of the complex pyrolysis model would provide the best representation of the flame spread than the simple burning model because the ignition temperature and HRRPUA for a given material are dependent on the heat flux incident to the material, which can vary significantly in realistic fire scenarios. The complex pyrolysis model also allows for explicit modeling of cooling, and an attendant decreased burning rate, of a burning surface due to fire sprinkler suppression, which is an influencing factor that was investigated in this work. The various parameters that required definition for the truss wood and the sheathing material using the complex pyrolysis model were determined through a literature review and the Monte Carlo-style simulations described in the following section.

Because of the complexity of flame spread scenario from the 6<sup>th</sup> floor through the 7<sup>th</sup> floor to the attic space and throughout the entire attic, two distinct models were constructed to simplify the simulations. The first model included the 6<sup>th</sup> and 7<sup>th</sup> floor fire rooms as well as the open hatch in the ceiling of the 7<sup>th</sup> floor that provided access to the attic. The second high-resolution model included all the geometry in the attic as well as the ventilation openings that represented the passive roof ventilators. The heat release rate measured at the open hatch from the first model simulation was used as the time-dependent fire source input to the second model simulation. For all models described as high resolution, all mesh elements were cubic and defined with a cell side length of 0.1 m.

#### 5.1.1. Ignition and Fire Spread from 6<sup>th</sup> Floor to Attic Space

An image of the geometry of the model constructed to represent ignition of the fire in the 6<sup>th</sup> floor fire room, spread to the 7<sup>th</sup> floor, and spread through the open access hatch in the ceiling of the 7<sup>th</sup> floor fire room is provided in Figure 12. The geometry was defined with 21 meshes for a total of 585,092 elements.

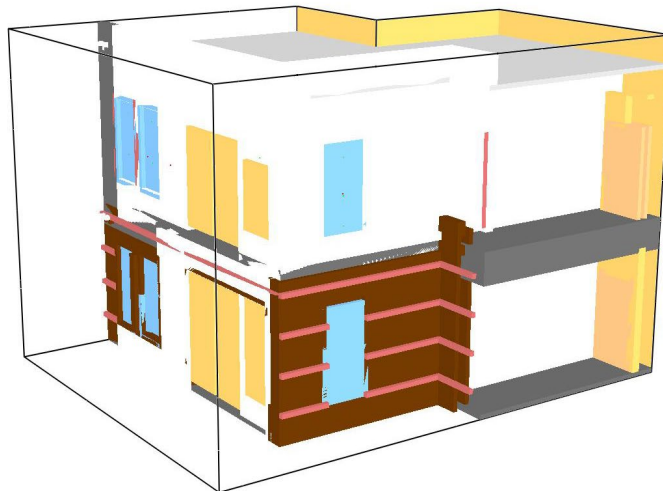


**Figure 12. Model constructed to simulate flame spread from 6<sup>th</sup> floor to attic space**

An opening in the ceiling of the 7<sup>th</sup> floor fire room with dimensions 1.2 m x 0.6 m that represented the open access hatch is shown in Figure 13. The size of the open access hatch was estimated based on photos taken at the scene by NIST personnel over several site visits. Wooden obstructions adjacent to the open access hatch that appeared charred in photographs were also defined in the model. Some of these wood obstructions are visible in Figure 13.

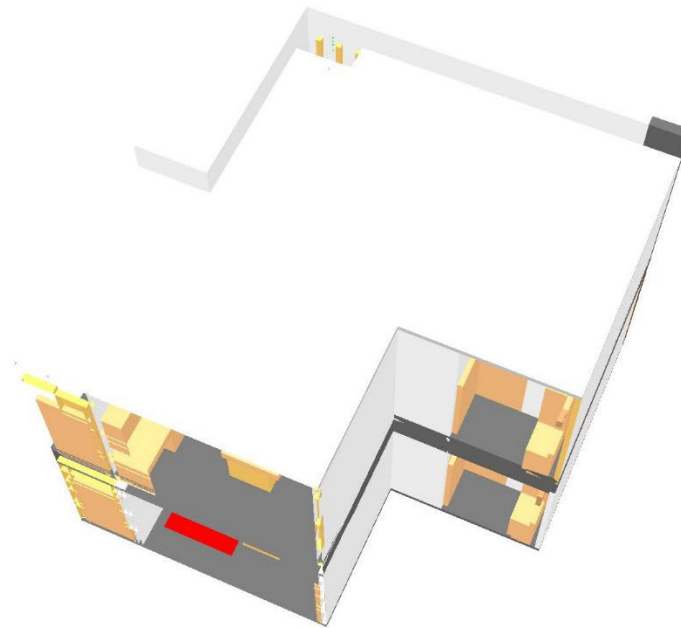


**Figure 13. Upper boundary of modeled geometry showing the open attic access hatch**

A plan view of the 6<sup>th</sup> floor apartment where the fire started is shown in Figure 14 and a plan view of the modeled 7<sup>th</sup> floor apartment is shown in Figure 15. The red rectangle shown in the figure is the source fire defined in the general vicinity of a pile of paper- and plastic-based trash. This source fire vent was defined with dimensions 1.5 m x 7.0 m. The source fire was defined to increase according to a fast, t-squared rate of increase over 134 s at which point the HRRPUA was 800 kW/m<sup>2</sup>, for a total heat release rate of 8.4 MW for 1126 s. This fire size was chosen as a ventilation-limited fire scenario based on visual evidence of the fire in the 6<sup>th</sup> floor apartment with a duration that was defined based on firefighter suppression efforts.

The blue obstructions shown on the bottom and right side of the modeled geometry indicate window coverings. Windows were not installed in the apartment complex at the time of the fire, but photographs from the scene prior to the fire spread appear to show plastic coverings over the windows. To simulate the effect of these coverings on ventilation to the fire and failure of these coverings to allow ventilation, the window coverings were defined to disappear from the model when temperature devices adjacent to the coverings reached a threshold value of 200°C.

Two construction doors installed on the south sides of 6<sup>th</sup> and 7<sup>th</sup> floor apartments were represented as obstructions with dimensions 0.9 m x 2.1 m x 0.1 m with a 0.1 m opening at the top and bottom, and between each door to represent the imperfect seal between the two doors on each level at the time of the fire. All of these doors were defined as combustible with the properties of the sheathing material assigned to the obstructions. The construction doors fell from the apartment building after thermal damage compromised the structure of the doors and the hinges that held the doors to the building. Because this effect could not be directly modeled adequately, the doors were defined to be removed from the simulation at a time that corresponded to the observations of the same phenomenon during the event.

The door to the bedroom on the southwest side of the 6<sup>th</sup> floor was defined to be open in the model due to the observation that flames apparently spread to the bedroom and extended out of the bedroom windows during the event. A portion of the eastern wall of the 6<sup>th</sup> floor apartment that had exposed wood studs was represented in the model with obstructions defined with typical thermo-physical properties and reaction parameters of lumber.

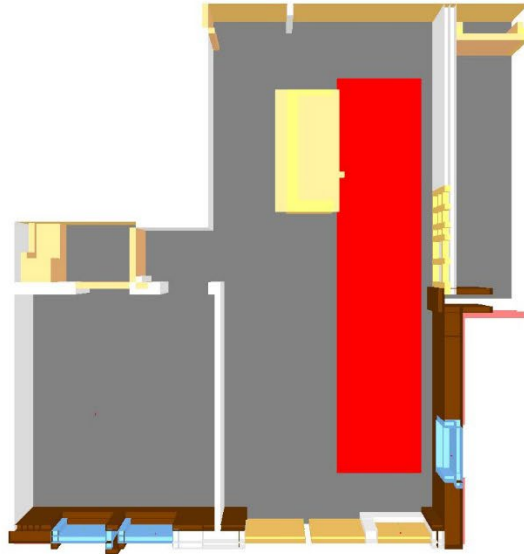


**Figure 14. Plan View of 6th Floor Geometry Modeled in High-Resolution Model**



**Figure 15. Plan View of 7<sup>th</sup> Floor Geometry Modeled in High-Resolution Model**

#### 5.1.2. Fire Spread through the Attic

The attic geometry was imported into Pyrosim® from Revit® and the geometry of the outer building envelope was assumed to be an accurate representation of the building on the day of the incident. The modeled geometry representing the attic space is visualized in Figure 16 and Figure 17. The Revit model represented locations of passive ventilators, but did not represent the trusses, mineral wool insulation, or locations of other obstructions in the attic. The roof of the attic had a slope that was expected to influence the flame and smoke spread through the attic. The slope of the roof was represented as a gradual increase to conform to the rectilinear mesh and these gradual increases in elevation from the central courtyard toward the outside of the modeled building are evident in Figure 16. The geometry was defined with 64 meshes with a total of 7,548,858 elements.

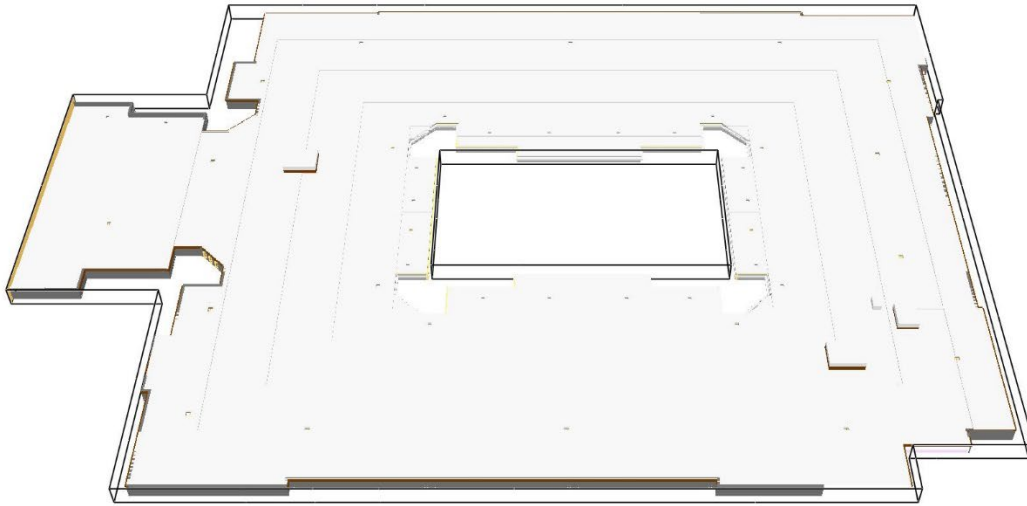


**Figure 16. Modeled geometry for the high-resolution attic space model**

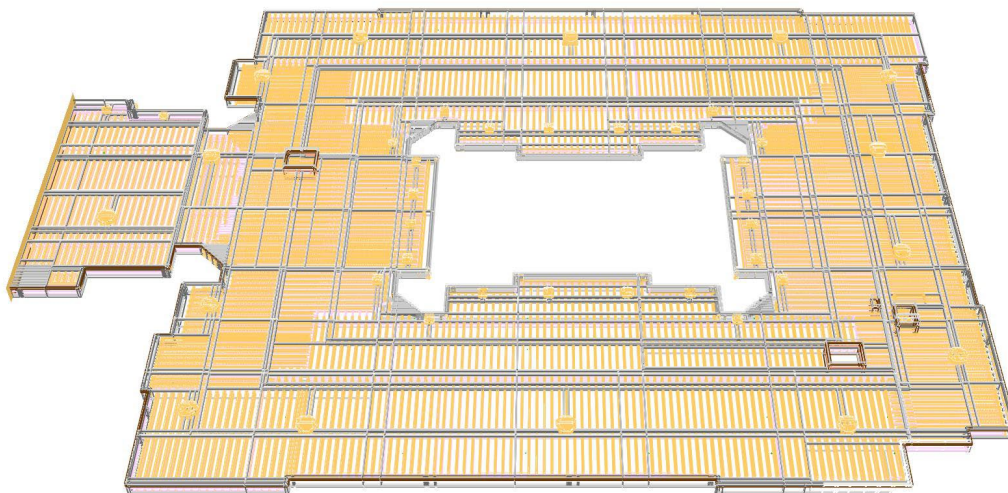


**Figure 17. Modeled geometry for the high-resolution attic space model represented with wireframe visualization**

The geometric representation of the trusses and the configuration of the trusses and insulation are visible in Figure 18. The trusses were represented as obstructions that conformed to the rectilinear mesh with all elements perpendicular to each other. The locations and total exposed area of the trusses were extracted from drawings provided to JENSEN HUGHES by NIST personnel. The height of the mineral wool insulation was defined as 0.3 m to agree with the installation of the insulation that was visible in site visits by NIST personnel. The total cross-sectional area of the holes cut into the upper boundary of the attic for the passive ventilators were defined based on the specifications for the ventilators.

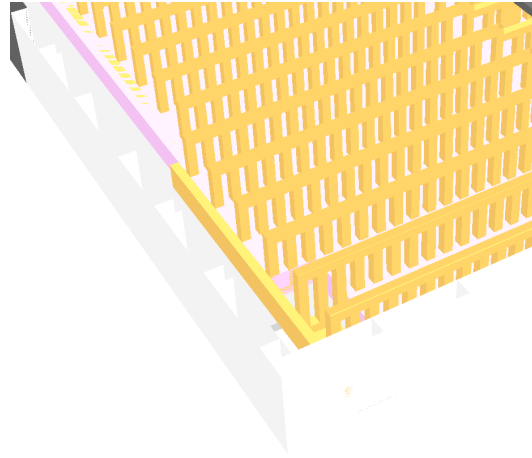


**Figure 18. Representation of Trusses and Insulation in Attic Space**

The fire source in the high-resolution attic model was represented as a vent with an area of 1.2 m x 0.6 m that had the HRRPUA measured at the open access hatch in the simulation that modeled ignition and fire spread to the attic. Modifications were made to the baseline model in the attic to investigate the effect of sprinklers and partitions on fire spread. The sprinklers were assigned properties explicitly defined in construction drawings and schedules from the FUSE 47 building, when available, and generic sprinkler properties otherwise. The sprinkler properties are presented in Table 4.

**Table 4. Sprinkler Properties Assigned to Attic Sprinklers**

Parameter	Definition	Source
Activation Temperature	93.3°C	Construction Drawings
RTI	50 m-s <sup>1/2</sup>	Assumed
Flow Rate	56.8 L/min	Construction Drawings
IOR	3	Construction Drawings
Spray Angle	20.0°, 80.0°	Assumed

Two modifications to the baseline high-resolution model that included partitions in the attic featured partitioned areas of 3,000 sq. ft. and 10,000 sq. ft. An image of these partitioned areas is provided in Figure 19. The partitions were assigned the properties of gypsum wallboard and there was no mechanism in place to allow fire to pass through these partitions. In Figure 19, the 3,000 sq. ft. partitioned area is outlined in red and the 10,000 sq. ft. area is outlined in yellow. Results of the simulations of high-resolution models with modifications are presented in Section 6.3.

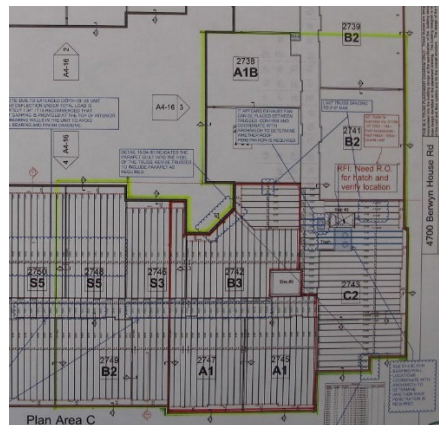


**Figure 19. Floorplan showing locations of gypsum wallboard partitions for 3,000 sq. ft. and 10,000 sq. ft. areas**

## 5.2. Monte Carlo Simulations

A Monte Carlo analysis is a statistical technique that can be used to evaluate a large number of parameters and their relationships to each other within a numerical model. With a large sample of simulations, this technique can identify which parameters are most significant for a given model, and the sensitivity of the model results to changes in each parameter.

The first step of applying a Monte Carlo analysis to a fire model involves identifying the parameters that may have some impact on the model results. A range of potential values must be assigned to each of these parameters; these ranges were specified as minimum and maximum bounds depending on the level of data that is available. For the Fuse 47 model, the following parameters and potential input ranges have been identified, as shown in Table 5. Several set of Monte Carlo simulations were conducted to gradually effectively narrow these ranges to generate results that more closely agreed with the observations that served as calibration conditions.

**Table 5. Model parameters adjusted in Monte Carlo-style simulations**

Parameter	Units	Minimum	Maximum	Reference
Grid Size	m	0.075	0.1	N/A
Soot yield	g/g	0.1	0.25	[2]
CO yield	g/g	0.005	0.0115	[2]
Source Fire Maximum HRRPUA	kW/m <sup>2</sup>			Modeled
Burn away	-	TRUE or FALSE		N/A
Wood thermal conductivity	W/m <sup>2</sup> -K	0.06	0.2	[3–9]
Wood specific heat	kJ/kg-K	1.4	2.2	[3, 4, 8, 10]
Wood density	kg/m <sup>2</sup>	200	600	[6]
Wood pyrolysis Arrhenius pre-exponential factor	1/s	1.13E2	3.96E16	[5, 7, 11–17]
Wood pyrolysis activation energy	kJ/mol	4.38E4	2.26E5	[5, 7, 11–17]
Wood pyrolysis heat of reaction	kJ/kg	150	10000	[5, 7, 16, 17]
Wood pyrolyzate heat of combustion	kJ/kg	12000	25000	[2]
Wood absorption coefficient	1/m <sup>2</sup>	1000	50000	Assumed
Wood emissivity	-	0.82	0.9	Assumed
Truss surface definition thickness	m	0.038	0.08	Assumed
Insulation thermal conductivity	W/m <sup>2</sup> -K	0.035	0.045	[18]
Insulation specific heat	kJ/kg-K	0.8	1.03	[18]
Insulation density	kg/m <sup>2</sup>	8	48	[18]
Insulation emissivity	-	0.7	0.92	Assumed
Insulation absorption coefficient	1/m <sup>2</sup>	800	50000	Assumed

The impact of changes in parameter values can be compared to outputs of interest through a correlation. In the case of this model, the outputs of interest have been identified as:

1. Maximum heat release rate
2. Time at which the temperature near the vent exceeds 500°C
3. Heat release rate when the temperature near the vent exceeds 500°C

Microsoft Excel was used to calculate the correlation between the input parameters and the outputs from the model. This function, CORREL provides a correlation coefficient,  $c$ :

$$c = \frac{\sum(x - \bar{x})(y - \bar{y})}{\sqrt{\sum(x - \bar{x})^2 \sum(y - \bar{y})^2}}$$

Where  $\bar{x}$  and  $\bar{y}$  are the sample means of the input parameter and output result arrays for the full set of simulations. The value of  $c$  will be between -1 and 1, where 0 has no correlation, and the significance of the correlation increases as  $c$  approached -1 (an inverse correlation) or +1 (a positive correlation).

The relationship between the number of simulations,  $n$ , and the statistical significance of the correlation coefficient,  $c$ , can be determined through an equation provided by Hald [19]:

$$t = \frac{c}{\sqrt{1-c^2}}(\sqrt{n-2})$$

Where  $t$  is the desired confidence level, which is typically chosen as 0.95 [20]. By solving this equation for  $c$ , one can determine the correlation coefficient that is statistically significant for the number of simulations and the desired confidence level.

A subsection of the attic space domain was defined as the domain for the Monte Carlo simulations to facilitate the high number of permutations of parameters required for statistical significance. This subsection included the vent that represented the open access hatch from the 7<sup>th</sup> floor apartment to the attic, several trusses, insulation, and an opening in the roof to represent one passive ventilator. The exterior walls of the building that coincided with this domain were included in the models, and the boundaries that corresponded to additional space in the attic were represented with open boundary conditions. Images of the domain defined for the Monte Carlo simulations is provided as Figure 20. The maximum HRR of the source fire was defined as a parameter investigated in the Monte Carlo simulations, although the time-dependent evolution of the source HRR was defined according to the measurement from the case that simulated ignition and spread of flame from the 6<sup>th</sup> floor to the attic.

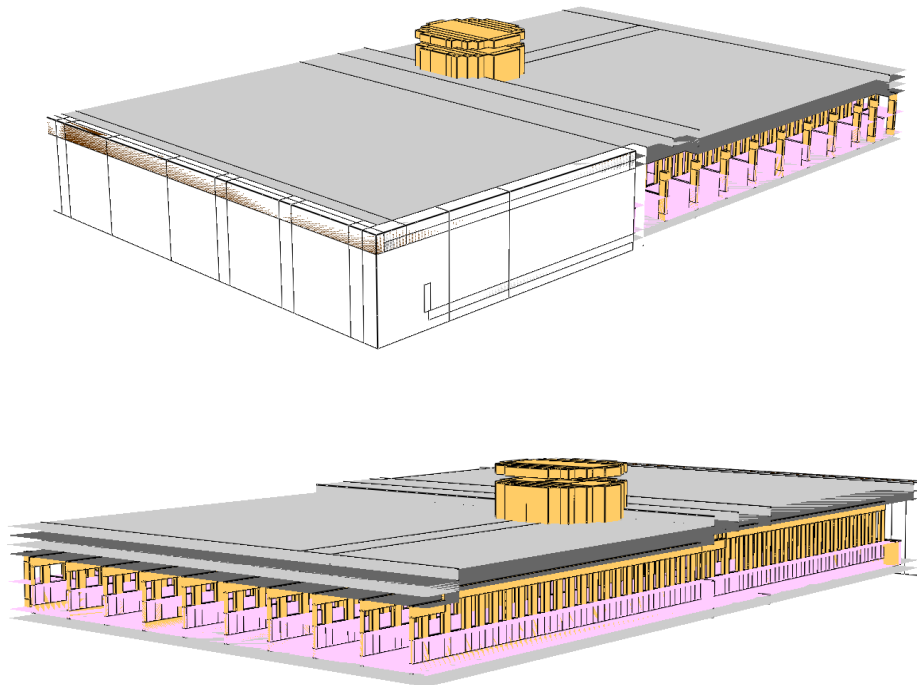


**Figure 20. Images of domain defined for Monte Carlo simulations**

The Monte Carlo simulations were defined to stop when the gas temperature in the modeled ventilator exceeded 500°C, which was taken to indicate that flames were venting at the ventilator. The time at which the simulations were stopped was compared to the observations of flames at the roof of the building on the day of the fire.

### 5.3. Low-Resolution Simulations

Several low-resolution models were constructed to investigate the effects of sprinklers and the presence of gypsum board on wall studs on flame spread and fire growth in a building under construction in various stages of completeness. These low-resolution models included geometric representations of the framing, floor support trusses, and combustible sheathing in the floor assembly for the 6<sup>th</sup> floor of the FUSE 47 building, which was typical for floors 3 through 6. The material properties for the wood trusses and sheathing were generally taken from the validated simulations of spread through the attic, although any deviations from this set of properties are explained in Section 6.3. For all of the low-resolution models, the entire eastern wing of the 6<sup>th</sup> floor was represented. The source fire for all low-resolution model simulations was defined as a vent with dimensions 1.5 m x 7.0 m that had the same maximum HRRPUA (800 kW/m<sup>2</sup>) and HRR evolution as was described for the model that represented ignition and spread from the 6<sup>th</sup> floor to the attic. All cubic grid cells were used in the mesh with a side of 0.2 m. All of the low-resolution simulations were meshed with 22 meshes for a total of 2,411,094 elements. The following sections describe the major configurations of the low-resolution model that were simulated in this work.

#### 5.3.1. Baseline Model

The baseline low-resolution model included finished exterior walls with no windows installed. None of the interior walls were defined as finished in this configuration and a geometric approximation of the interior framing was included for all walls. This model was also constructed assuming there was no ceiling installed, so the structural floor trusses and the sheathing in the floor assembly for the next highest floor were represented and defined as combustible. Because the grid resolution was relatively low, accurate spacing of wall studs could not be achieved and the total surface area of the wood members was estimated and accurately represented. An image of the baseline model is provided in Figure 21. All the boundaries shown in the figure were defined with open boundary conditions.

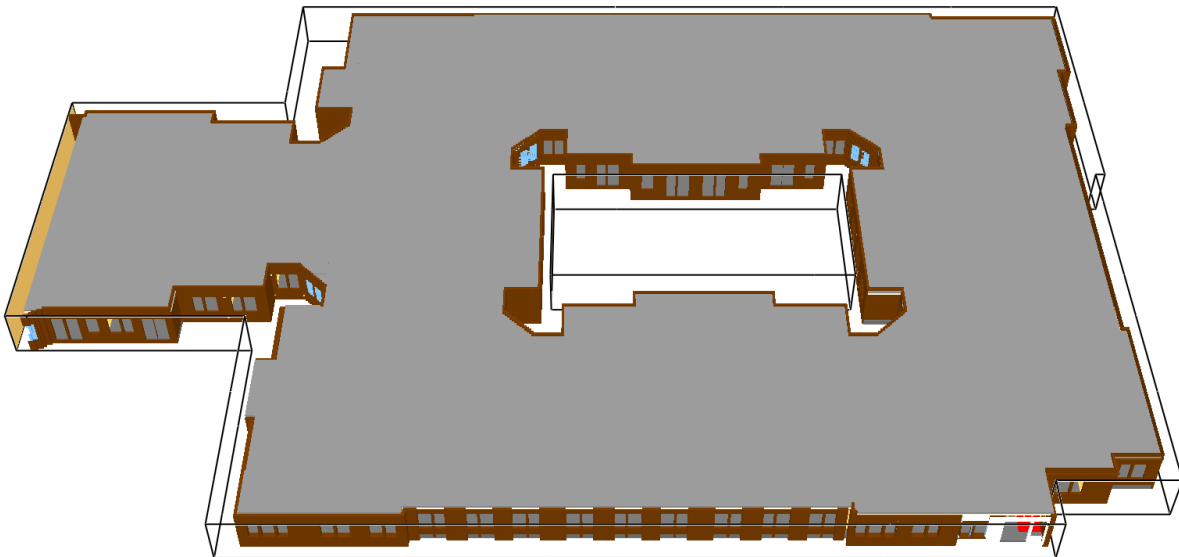


**Figure 21. Image showing boundaries and construction of low-resolution baseline model**

The typical representation of construction of the wood framing in the low-resolution model is shown in the image provided as Figure 22. Wood framing for walls is represented as close to physical dimensions as possible. For simplicity and because obstructions in FDS must adhere to the rectilinear mesh, the structural flooring wood trusses are defined as an array of single obstructions above the finished ceiling level. The combustible sheathing from the bottom layer of the flooring assembly for the above floor is represented in this figure as a plane with a light gray color, but has a thickness of one grid cell in the simulation and is located adjacent to the obstructions representing the structural floor trusses.

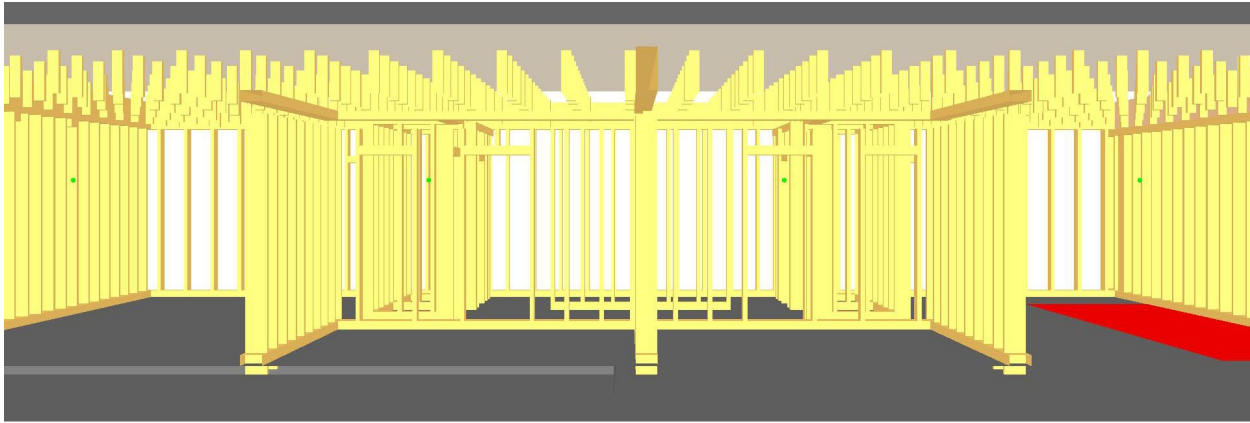


**Figure 22. Typical representation of construction in the low-resolution models**

Two models with modifications were also constructed for this configuration. One model included pendant sprinklers that were installed for the living spaces in the apartments throughout the modeled level as well as upright concealed space sprinklers that were installed between the floors. The sprinklers were assigned properties explicitly defined in construction drawings and schedules from the FUSE 47 building, when available, and generic sprinkler properties otherwise. The properties of the sprinklers defined in the modified low-resolution model are provided in Table 6 and Table 7.

**Table 6. Pendant sprinkler properties defined in modified low-resolution model**

Parameter	Definition	Source
Activation Temperature	74.0°C	Construction Drawings
RTI	150 m-s <sup>1/2</sup>	Assumed
Flow Rate	96.9 L/min	Construction Drawings
IOR	-3	Construction Drawings
Spray Angle	25.0°, 80.0°	Assumed

**Table 7. Upright concealed-space sprinkler properties defined in modified low-resolution model**

Parameter	Definition	Source
Activation Temperature	74.0°C	Construction Drawings
RTI	150 m-s <sup>1/2</sup>	Assumed
Flow Rate	96.9 L/min	Construction Drawings
IOR	3	Construction Drawings
Spray Angle	20.0°, 75.0°	Assumed

The second model modification included gypsum wall board installed to create a 10,000 sq. ft. partition in the baseline model. The partitioned area for the modified low-resolution model is outlined in red in Figure 23.

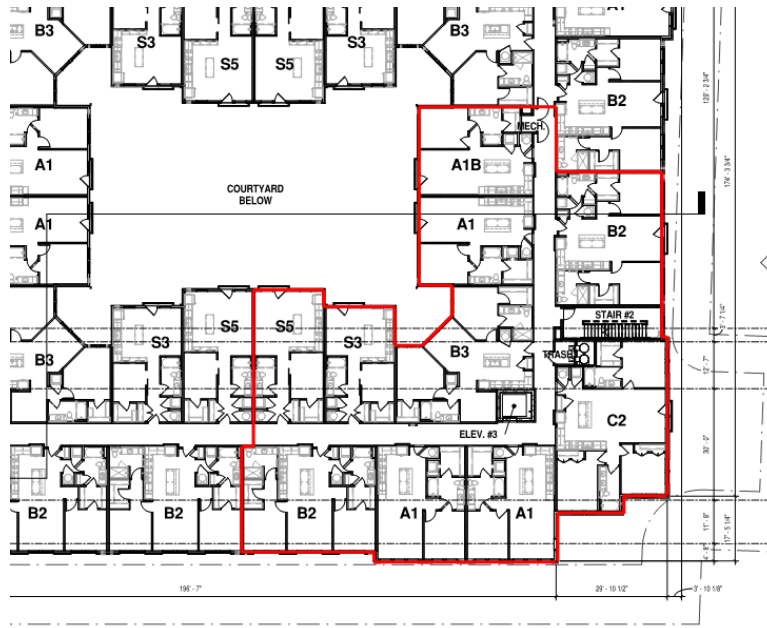


**Figure 23. 10,000 sq. ft. area partitioned for modified low-resolution model**

5.3.2. Baseline Model with Exterior Walls Removed

The baseline low-resolution model with the exterior walls removed is identical to the baseline low-resolution with the finished walls replaced by wood stud framing. The only scenario simulated in this configuration was the case where no partitions or sprinklers are included in the model. Images of the model are presented in Figure 24 and Figure 25.

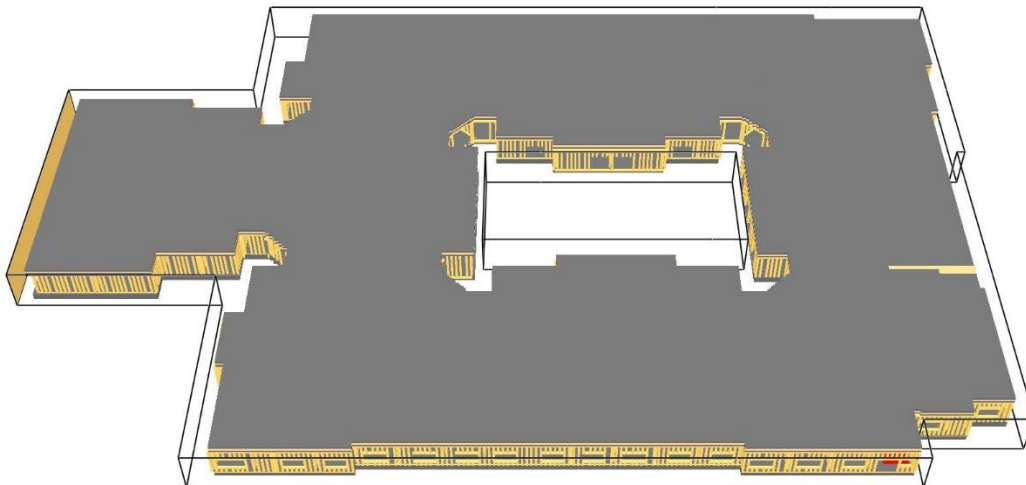


**Figure 24. Image showing boundaries and construction of low-resolution baseline model with the exterior walls removed**

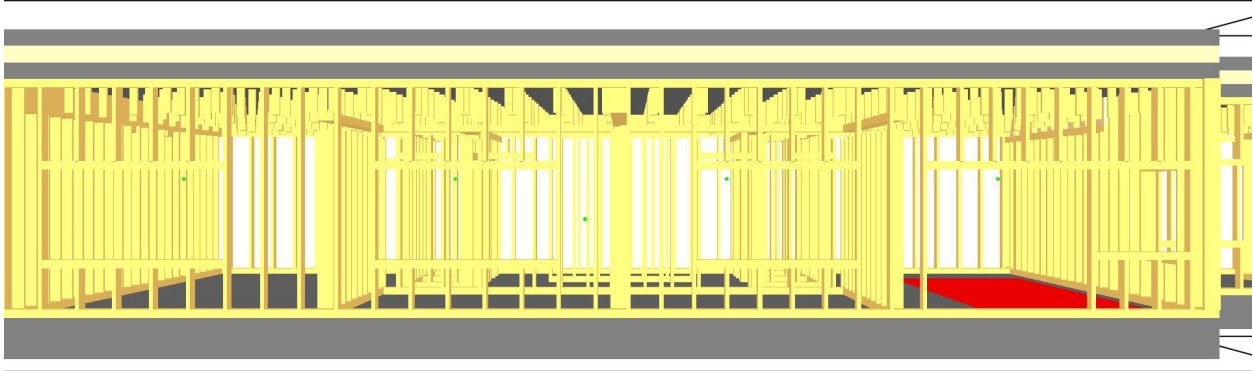


**Figure 25. Typical representation of construction in the low-resolution model with the exterior walls removed**

## **6. RESULTS**

The results of all completed simulations are presented in the following subsections. A comprehensive list of the FDS input and output files submitted to NIST that correspond to those discussed in this section are listed in Appendix A.

### **6.1. Ignition and Spread from 6<sup>th</sup> Floor to Attic Space**

In the simulation for ignition in the 6<sup>th</sup> floor and fire spread through the 7<sup>th</sup> floor open access hatch in the to the attic, it is evident that the source fire quickly causes failure of the window on the eastern side of the apartment and ignites the exposed wood studs in the wall, as seen in Figure 26. Shortly after ignition of the studs and prior to the source fire achieving its maximum HRR, it is evident in Figure 27 that the flames are visible at the upper interface between the two construction doors. This image appears similar to the photograph captured when firefighters first arrived at the Fuse 47 fire shown in Figure 1.

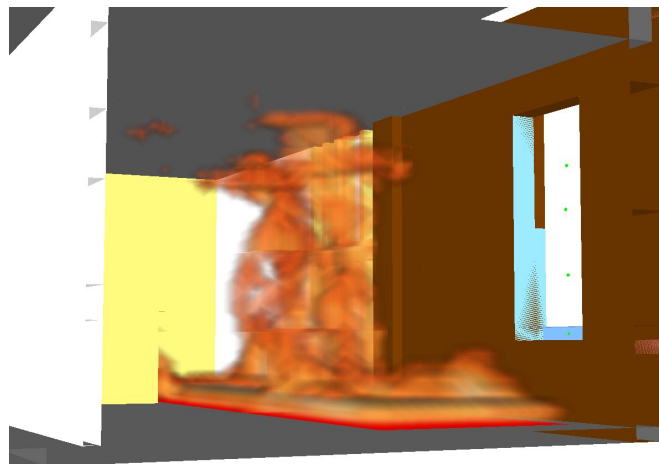


**Figure 26. Image from ignition simulation showing flames attached to the exposed wood studs and the open window on the east side of the apartment**

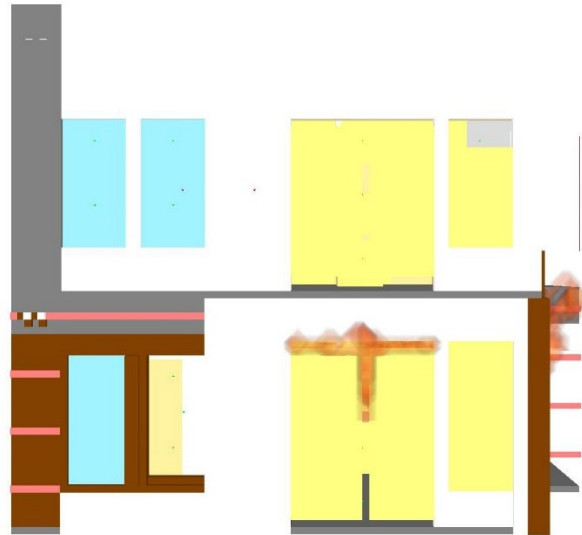


**Figure 27. Ignition and Spread from 6th floor to Attic simulation showing flames at construction doors on 6th floor**

As the source fire reached its maximum HRR and the exposed wood studs were also burning, large flame extensions were visible in the FDS simulation from between the construction doors and the window on the 6<sup>th</sup> floor. This is captured in the image provided as Figure 28 where there is also some burning visible on the outside of the 7<sup>th</sup> floor construction doors. Shortly after these large flame extensions are visible from the 6<sup>th</sup> floor, the construction doors on the 6<sup>th</sup> floor are removed from the simulation to simulate the time when the construction doors fell from the building. It is evident that significant burning and flame extension still occurs after the construction doors fall off the building, although the construction doors no longer act as a fuel source for the fire.

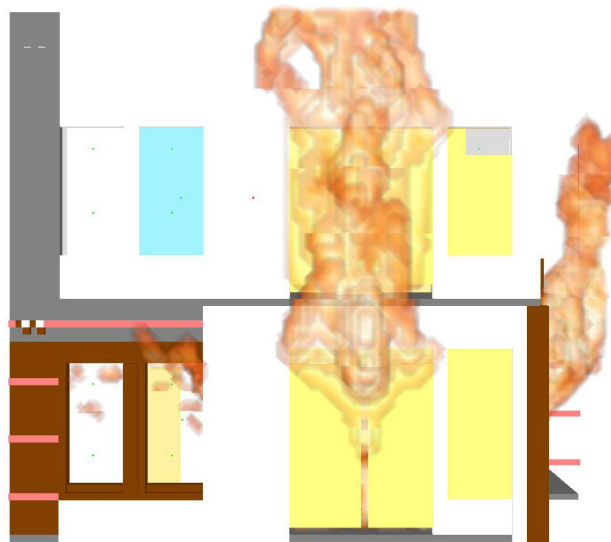


**Figure 28. Image showing flames extending out of 6<sup>th</sup> floor construction doors and window**



**Figure 29. Image showing flames extending out of 6th floor apartment after construction doors have fallen off building**

An image from inside of the 7<sup>th</sup> floor apartment at a point when flames were extending from through the open access hatch in the ceiling of the apartment is provided in Figure 30. This image shows that the simulation predicts that the mechanism that allowed the fire to spread from the 6<sup>th</sup> floor to the attic was ignition of exposed wood members in the 7<sup>th</sup> floor that were immediately adjacent to the open access hatch. While the 7<sup>th</sup> floor construction doors were exposed to heat from the flames extending from the 6<sup>th</sup> floor, minor burning of the 7<sup>th</sup> floor doors occurred and facilitated ignition of the exposed wood studs above the 7<sup>th</sup> floor construction doors. This simulation indicates that the fire that ignited the wood trusses in the attic space passed through the open access hatch while the 6<sup>th</sup> floor and 7<sup>th</sup> floor construction doors were still intact and attached to the building. This agrees with observations made at the scene during the incident because water suppression was applied to the 6<sup>th</sup> floor apartment after the 6<sup>th</sup> floor construction doors fell off the building, which reduced the flame extension from the 6<sup>th</sup> floor and effectively reduced heat flux from the flames to the 7<sup>th</sup> floor apartment.

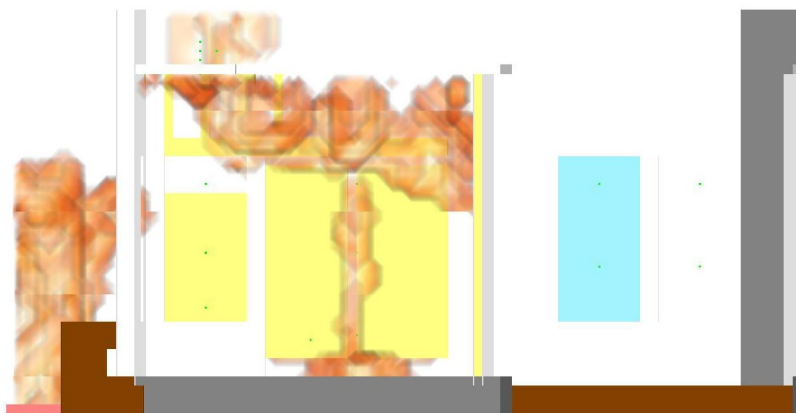


**Figure 30. Flame spread in 7th floor apartment showing exposed wood burning and flames extending through the open access hatch to attic**

A plastic trash can that remained in the 7<sup>th</sup> floor apartment throughout the fire event and sustained minimal thermal damage provided a data point in the comparison between the FDS simulation and the

real event. The trash can appeared to made of polyethylene. Pure high-density polyethylene (HDPE) has an approximate melting temperature of 137°C, although the melting temperature of commercial available products is likely higher due to addition of plasticizers, dyes, and other chemicals to the HDPE during production. The gas temperature measured at the approximate position of the upper edge of the trash can has been plotted in Figure 31 along with a line indicating the melting temperature of pure HDPE. It is evident that the gas temperature briefly exceeds 137°C. It must be kept in mind that this is the free gas temperature and does not take into effect heat transfer to the solid HDPE trash can, so it is understood that the solid surface temperature would be lower than the gas temperature at this point. This evidence is compelling that the simulation results are feasible and the trash can in the assumed position would have experienced minor thermal damage.

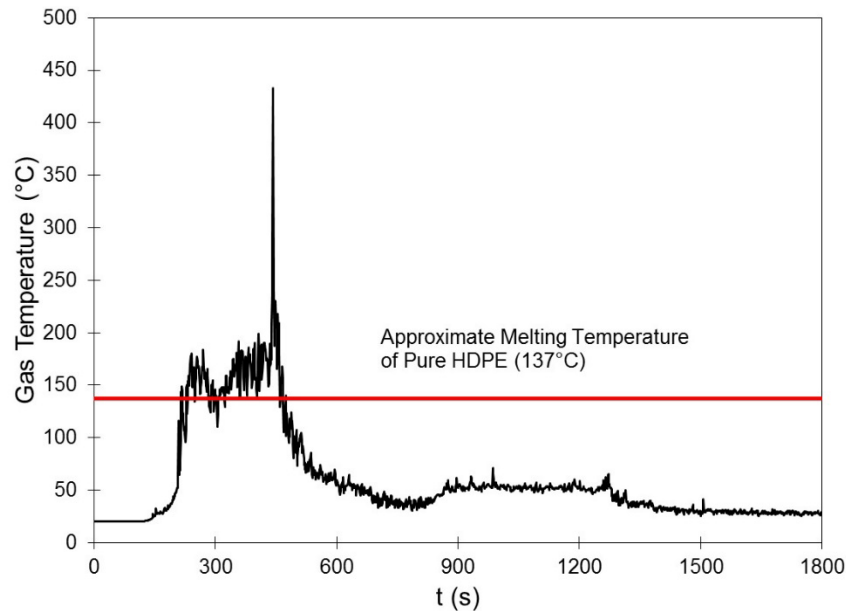


**Figure 31. Gas Temperature measured in approximate vicinity of trash can in FDS model**

The HRRPUA measured across the area of the open access hatch provides an area-averaged representation of the total heat energy that passes from the 7<sup>th</sup> floor to the attic space over the course of the fire event. This measurement is plotted in Figure 32. The exact profile measured in this simulation was passed to the Monte Carlo simulations and the fine-resolution attic fire spread model. It is evident when considering the data from Figure 31 and Figure 32 that all passage of flames from the 7<sup>th</sup> floor to the attic space occurred over a relatively short period of time shortly after flame extension out of the 6<sup>th</sup> floor apartment and prior to firefighter suppression efforts.

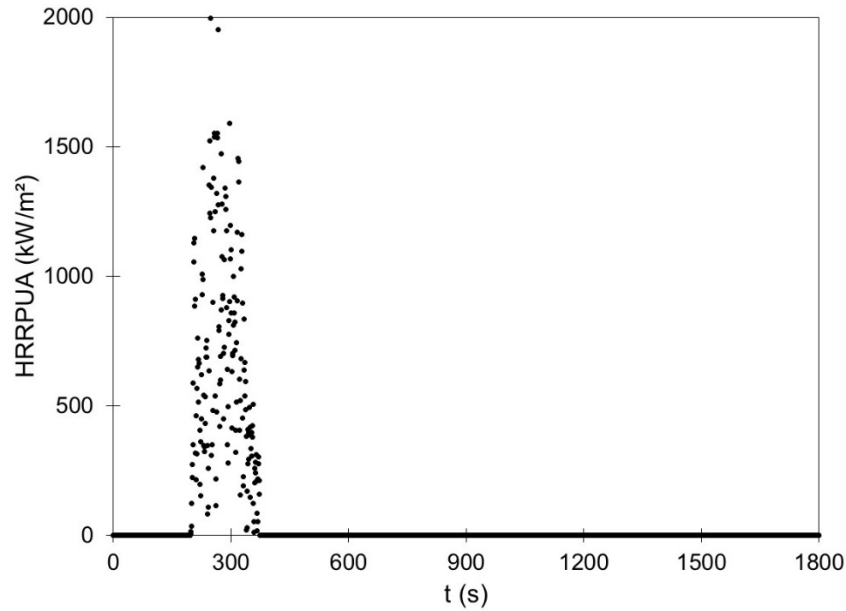


**Figure 32. HRRPUA measured at open access hatch to attic space over the duration of the simulation**

## 6.2. Monte Carlo Simulations

A total of  $n = 50$  simulations were run in the final configuration, using a fine-resolution model of the attic space above the area of origin. At a confidence level of 0.95, this equates to the correlation coefficient,  $c$ , being statistically significant when the absolute value of  $c$  is greater than 0.1358. A summary of the simulations that were run is provided in Table 8. The output parameters of interest are the Duration of Simulation, defined as the time at which the temperature in the ventilator indicated flame extension at that point, the Total HRR at the End of the simulation, whether the end of the simulation was the specified duration or the simulation was ended early due to flame extension at the ventilator, the Maximum Total HRR.

The simulations were defined with a total duration of 1800 s, which is the approximate amount of time between observation of flames in the attic and observation of flames at the roof of the building. Higher values of this output quantity are considered closer to the real scenario as long as the HRR at end of the simulation indicates that the fire is still active. For the results presented in Table 8, when the HRR at the end of the simulation was significantly lower than the maximum total HRR (less than 50%), it was a good indication that the unique set of parameters defined in the simulation would not facilitate fire growth and flame spread.

Table 8. Input parameters for Monte Carlo simulations

	Grid Size (m)	HRRPUA (kW/m <sup>2</sup> )	SOOT YIELD (g/g)	CO YIELD (g/g)	BURN AWAY	Char Yield (g/g)	Char Density (kg/m <sup>3</sup> )	Thermal Conductivity (W/m <sup>2</sup> K)	Specific Heat (kJ/kgK)	Density (kg/m <sup>3</sup> )	Heat of Reaction (kJ/kg)	Heat of Combustion (kJ/kg)	Absorption Coefficient (1/m <sup>2</sup> )	Emissivity	Arrhenius Pre-Exponential Factor (1/s)	Activation Energy (J/mol)	Wood Stud Thickness (m)	Insulation			Output				
																		Thermal Conductivity (W/m <sup>2</sup> K)	Specific Heat (kJ/kgK)	Density (kg/m <sup>3</sup> )	Absorption Coefficient (1/m <sup>2</sup> )	Emissivity	Duration of Simulation (s)	Total HRR at End of Simulation (kW)	Maximum Total HRR (kW)
1	0.075	1646	0.013	0.008	TRUE	0.372	161.3	0.60	1.5	433.7	1075	16078	58375	0.86	4.33E+15	1.81E+05	0.035	0.04	0.8	32	43615	0.89	1800	0	656
2	0.075	1884	0.010	0.007	FALSE	0.389	180.5	1.09	1.9	464.2	2966	13526	35972	0.81	2.54E+08	9.07E+04	0.039	0.10	0.9	27	40043	0.78	1800	1	536
3	0.1	1754	0.011	0.006	FALSE	0.057	29.8	0.39	2.0	527.2	404	12324	45218	0.88	8.29E+12	1.47E+05	0.031	0.10	1.1	20	48776	0.84	1800	0	253
4	0.1	1855	0.008	0.006	TRUE	0.093	35.2	0.72	1.5	378.9	1659	12503	57569	0.87	3.48E+15	1.80E+05	0.022	0.05	1.2	42	69845	0.83	1800	0	282
5	0.075	1571	0.005	0.008	TRUE	0.352	114.7	0.99	1.9	325.3	1595	17464	40395	0.84	1.98E+16	2.90E+05	0.020	0.05	0.9	20	53188	0.88	1800	0	665
6	0.1	1538	0.009	0.006	FALSE	0.253	94.1	0.17	1.6	372.0	1548	12298	37356	0.81	1.41E+08	8.75E+04	0.042	0.07	1.2	32	66002	0.80	1800	1	239
7	0.075	1863	0.007	0.005	TRUE	0.406	236.7	0.23	1.5	582.6	937	14119	53008	0.90	3.39E+05	5.47E+04	0.040	0.04	0.8	21	59269	0.85	67	1510	1510
8	0.1	2192	0.012	0.004	FALSE	0.500	205.1	0.28	1.8	410.5	3263	16654	61209	0.86	6.92E+05	5.86E+04	0.030	0.07	1.0	26	50431	0.83	70	1748	1748
9	0.1	1849	0.013	0.006	TRUE	0.175	98.6	1.07	1.6	562.8	846	13807	54899	0.86	1.58E+13	1.51E+05	0.029	0.09	0.9	22	36828	0.78	1800	0	503
10	0.075	1918	0.009	0.004	FALSE	0.283	122.3	1.11	1.9	431.7	2143	13573	40323	0.81	4.02E+10	1.18E+05	0.033	0.05	1.1	20	42751	0.79	1800	0	559
11	0.1	2377	0.013	0.003	FALSE	0.252	112.6	0.85	2.0	446.6	3376	15281	39491	0.86	2.16E+11	1.27E+05	0.031	0.07	0.9	36	45821	0.85	1800	0	715
12	0.075	1621	0.014	0.008	FALSE	0.434	174.0	0.36	1.5	400.6	508	15923	35462	0.87	1.41E+15	1.75E+05	0.030	0.09	1.1	45	43367	0.88	61	1562	1562
13	0.1	1882	0.010	0.006	TRUE	0.325	157.8	0.72	1.9	485.3	763	13440	62220	0.89	1.12E+13	1.49E+05	0.042	0.07	0.8	21	58508	0.90	1800	0	443
14	0.075	1559	0.005	0.003	FALSE	0.096	52.3	0.19	1.7	545.4	2360	15112	58898	0.88	6.91E+06	7.11E+04	0.044	0.09	1.1	31	63013	0.81	61	1592	1592
15	0.1	1757	0.013	0.008	FALSE	0.319	146.3	0.51	1.4	458.1	1128	14590	56274	0.84	6.21E+13	1.58E+05	0.015	0.05	1.2	19	37925	0.81	259	1231	1239
16	0.1	1596	0.006	0.007	FALSE	0.599	278.4	0.53	1.6	464.4	1160	16207	46710	0.89	9.07E+18	2.23E+05	0.035	0.08	1.0	37	53121	0.78	1800	0	703
17	0.075	1989	0.014	0.007	TRUE	0.262	114.6	0.47	1.5	438.2	2310	14258	36256	0.90	1.27E+17	2.00E+05	0.021	0.07	1.0	20	39048	0.84	1800	0	605
18	0.1	1603	0.011	0.005	FALSE	0.139	72.1	1.11	1.9	519.1	3186	17278	53363	0.83	1.69E+06	6.34E+04	0.040	0.08	0.9	17	42509	0.81	59	1713	1713
19	0.1	2016	0.011	0.006	TRUE	0.108	53.1	0.82	1.8	491.6	1928	15927	32752	0.80	2.03E+09	1.02E+05	0.027	0.09	1.2	47	43006	0.83	1800	7	861
20	0.075	1497	0.006	0.005	TRUE	0.432	186.8	0.38	1.5	432.0	1885	17662	48297	0.85	2.46E+17	2.03E+05	0.034	0.05	1.2	38	56872	0.79	1800	0	551
21	0.1	1466	0.012	0.008	TRUE	0.309	155.4	0.90	1.6	502.6	3219	12007	54087	0.80	1.93E+10	1.14E+05	0.029	0.07	1.0	41	61390	0.80	1800	0	197
22	0.075	2048	0.010	0.004	FALSE	0.284	101.6	0.72	1.6	357.5	1051	16593	39714	0.87	1.01E+18	2.11E+05	0.021	0.04	0.9	34	51864	0.85	77	1682	1682
23	0.075	2018	0.011	0.009	FALSE	0.191	70.9	0.83	1.5	370.9	1687	15972	54292	0.81	1.61E+11	1.26E+05	0.038	0.08	0.9	29	63317	0.88	94	1703	1703
24	0.1	1493	0.014	0.005	TRUE	0.110	64.2	0.21	1.6	581.9	1975	15884	49179	0.86	9.08E+13	1.60E+05	0.031	0.07	1.1	48	34232	0.78	1800	0	606
25	0.1	1929	0.009	0.008	TRUE	0.458	265.4	0.89	1.8	579.9	2482	12563	37681	0.90	4.79E+06	6.91E+04	0.031	0.10	1.0	32	56857	0.81	1800	12	320
26	0.075	1620	0.011	0.005	FALSE	0.199	74.1	0.88	1.4	372.8	2617	14368	57512	0.84	7.67E+09	1.09E+05	0.036	0.07	1.1	17	46972	0.80	1800	0	734
27	0.075	2378	0.014	0.005	FALSE	0.524	284.3	0.50	1.9	542.6	2798	17696	45096	0.88	6.34E+07	8.32E+04	0.025	0.07	1.1	43	36690	0.87	113	1737	1737
28	0.1	1485	0.011	0.004	TRUE	0.131	68.8	0.51	1.5	524.6	1939	12540	61599	0.88	1.96E+09	1.02E+05	0.018	0.08	0.8	32	49800	0.78	1800	0	263
29	0.1	2240	0.014	0.007	TRUE	0.366	206.4	0.94	1.7	563.7	2202	17940	30021	0.90	1.77E+17	2.01E+05	0.031	0.09	1.0	23	66034	0.82	1800	0	929
30	0.075	1632	0.007	0.007	TRUE	0.515	256.5	0.74	1.5	498.3	2726	15489	65630	0.87	8.84E+18	2.23E+05	0.043	0.04	1.0	20	49372	0.88	1800	0	515
31	0.075	1858	0.005	0.007	TRUE	0.345	154.0	0.14	1.6	446.9	641	13134	34923	0.82	4.45E+07	8.12E+04	0.016	0.05	1.1	33	49965	0.85	1800	483	636
32	0.1	2129	0.014	0.008	FALSE	0.562	263.9	0.31	1.6	469.5	3326	12492	46681	0.86	4.53E+07	8.13E+04	0.018	0.05	0.8	36	32083	0.84	1800	2	320
33	0.075	2237	0.014	0.009	FALSE	0.064	34.2	0.98	2.0	535.7	599	12185	37104	0.85	2.87E+10	1.16E+05	0.043	0.06	0.9	27	55928	0.82	1800	0	340
34	0.1	1528	0.008	0.006	FALSE	0.500	249.4	0.27	1.4	498.8	3461	15240	65939	0.83	2.39E+06	6.53E+04	0.036	0.06	1.2	29	60558	0.82	463	1311	1311
35	0.075	1635	0.006	0.006	TRUE	0.124	44.9	0.27	1.6	362.7	3206	12624	57016	0.89	2.97E+11	1.29E+05	0.037	0.07	1.1	22	41997	0.84	1800	0	321
36	0.075	2160	0.007	0.003	TRUE	0.328	186.7	0.10	1.7	569.2	1678	12610	33735	0.82	1.35E+09	9.98E+04	0.045	0.06	0.9	18	31854	0.79	1800	0	421
37	0.075	1707	0.006	0.008	FALSE	0.480	159.6	0.65	1.9	332.7	2650	12062	43524	0.88	8.62E+08	9.74E+04	0.016	0.08	1.1	33	58290	0.86	1800	0	184
38	0.1	2334	0.009	0.003	TRUE	0.489	235.9	0.44	1.9	482.4	1991	14911	34193	0.87	3.31E+06	6.71E+04	0.042	0.09	1.1	18	33541	0.76	1800	64	728
39	0.1	2004	0.012	0.004	FALSE	0.427	170.1	0.76	1.5	398.6	2629	13409	59965	0.87	1.39E+13	1.50E+05	0.037	0.10	1.2	19	44768	0.80	1800	0	472
40	0.075	1532	0.007	0.004	FALSE	0.273	113.7	0.30	1.9	416.5	1773	12911	39158	0.86	9.92E+13	1.61E+05	0.038	0.06	0.8	24	33660	0.83	1800	0	390
41	0.1	1468	0.008	0.007	TRUE	0.200	101.7	0.54	2.0	508.4	518	17603	47306	0.88	1.56E+14	1.63E+05	0.021	0.09	0.9	32	45840	0.87	85	1536	1536
42	0.075	1560	0.010	0.007	FALSE	0.120	63.6	0.42	1.4	531.8	459	12047	35013	0.87	3.57E+06	6.75E+04	0.028	0.09	1.1	33	55271	0.77	1800	1131	1148
43	0.1	2027	0.007	0.004	TRUE	0.141	51.7	0.42	1.6	365.3	2012	13107	65717	0.83	7.72E+14	1.72E+05	0.021	0.10	0.8	39	42537	0.83	1800	0	366
44	0.1	2228	0.008	0.005	FALSE	0.342	143.8	0.80	1.4	420.7	667	14288	46087	0.90	4.87E+13	1.57E+05	0.020	0.10	1.1	27	41766	0.85	275	1266	1266
45	0.075	2162	0.008	0.006	FALSE	0.182	85.2	0.46	1.7	467.5	568	12147	46973	0.87	8.03E+10	1.22E+05	0.024	0.08	0.9	47	48315	0.89	1800	0	272
46	0.1	1467	0.012	0.004	FALSE	0.424	154.1	0.57	1.8	363.6	698	15996	62943	0.81	1.61E+07	7.57E+04	0.042	0.08	1.0	21	51635	0.89	61	1628	1628
47	0.1	1678	0.006	0.006	FALSE	0.292	122.6	0.66	1.6	419.7	219	17542	37230	0.84	2.37E+08	9.03E+04	0.035	0.05	1.2	45	53096	0.87	38	1990	1990
48	0.1	2261	0.006	0.008	FALSE	0.083	40.9	0.83	1.8	492.6	1213	16887	45630	0.84	3.39E+16	1.93E+05	0.039	0.07	1.2	36	47759	0.89	117	1373	1425
49	0.075	2316	0.015	0.004	FALSE	0.196	81.5	0.72	1.8	416.															

The correlations between the input parameters that were varied in the Monte Carlo simulations and the output quantities that were used to compare simulations to each other and to the observations made at the scene at the time of the incident are presented in Table 9. A final output parameter that was considered in the Monte Carlo simulations was a binary indicator of whether or not the set of parameters defined facilitated flame spread. In the table, positive numbers correspond to a positive correlation between the input parameter and the output quantities, i.e. an increase in the input parameter corresponds to an increase in the output quantity. The correlation coefficients take on a value of 1 corresponding to a perfect positive linear correlation, 0 indicating no linear correlation, and -1 indicating a perfect negative correlation.

In Table 9, the correlations that are highest are highlighted in green, correlations that are statistically significant, but of less importance are highlighted in yellow, and the correlations that are not statistically significant are highlighted in gray. All output quantities that were considered are most sensitive to the BURN AWAY parameter and the heat of combustion. Other parameters that significantly affect the output include the insulation optical parameters, the reaction kinetics for the wood material, and the heat of reaction of the pyrolysis reaction. For the purposes of calibrating the model, the most important output quantities were first that the set of parameters facilitated flame spread, and then that the duration of the simulation was closest to the 1800 s reference point.

**Table 9. Correlations between input parameters and output quantities from Monte Carlo simulations**

Parameter	Duration of Simulation	Total HRR at End of Simulation	Maximum Total HRR	Flame Spread
Grid Size	0.041	0.007	-0.003	0.030
HRRPUA	-0.061	0.033	0.087	0.015
SOOT YIELD	-0.099	0.084	0.155	0.027
CO YIELD	0.099	-0.094	-0.142	-0.046
BURN AWAY	0.404	-0.422	-0.359	-0.385
Char Yield	-0.035	0.017	0.051	0.012
Char Density	-0.016	0.000	0.036	0.000
Wood Thermal Conductivity	0.040	-0.075	0.028	-0.135
Wood Specific Heat	0.021	-0.051	-0.014	-0.111
Wood Density	0.053	-0.037	-0.028	-0.013
Heat of Reaction	0.197	-0.236	-0.202	-0.285
Heat of Combustion	-0.565	0.534	0.716	0.452
Wood Absorption Coefficient	-0.118	0.056	-0.017	0.033
Wood Emissivity	0.043	-0.059	-0.045	-0.074
Arrhenius Pre-Exponential Factor	0.126	-0.135	-0.071	-0.142
Activation Energy	0.178	-0.260	-0.167	-0.267
Wood Stud Thickness	-0.001	-0.021	0.028	-0.100
Insulation Thermal Conductivity	0.036	-0.035	-0.039	-0.047
Insulation Specific Heat	-0.121	0.137	0.123	0.170
Insulation Density	-0.048	0.081	0.041	0.066
Insulation Absorption Coefficient	-0.316	0.268	0.252	0.256
Insulation Emissivity	-0.153	0.183	0.110	0.176

Because it was important to consider sets of parameters that facilitated flame spread, an additional analysis was conducted only considering the sets of parameters that resulted in flame spread to provide an understanding of the input parameters that influence the rate of flame spread the most given that flame spread occurs. The results of this analysis are provided in Table 10 and include  $n = 18$  simulations. At a confidence level of 0.95, this equates to the correlation coefficient,  $c$ , being statistically significant when the absolute value of  $c$  is greater than 0.231. The same coloring convention used in Table 9 was also used in Table 10.

**Table 10. Correlations between input and output parameters from Monte Carlo simulations when considering only simulations that promote flame spread**

Parameter	Duration of Simulation	Total HRR at End of Simulation	Maximum Total HRR
Grid Size	0.278	-0.123	-0.114
HRRPUA	-0.179	0.093	0.112
SOOT YIELD	-0.287	0.355	0.336
CO YIELD	0.241	-0.317	-0.315
BURN AWAY	0.285	-0.438	-0.421
Char Yield	-0.105	0.024	0.016
Char Density	-0.068	-0.015	-0.025
Wood Thermal Conductivity	-0.374	0.396	0.399
Wood Specific Heat	-0.329	0.352	0.383
Wood Density	0.171	-0.164	-0.178
Heat of Reaction	-0.228	0.224	0.219
Heat of Combustion	-0.761	0.757	0.780
Wood Absorption Coefficient	-0.357	0.173	0.149
Wood Emissivity	-0.102	0.072	0.042
Arrhenius Pre-Exponential Factor	-0.107	0.139	0.143
Activation Energy	-0.257	0.005	0.002
Wood Stud Thickness	-0.360	0.452	0.456
Insulation Thermal Conductivity	-0.026	0.054	0.036
Insulation Specific Heat	0.145	-0.195	-0.199
Insulation Density	0.056	0.137	0.164
Insulation Absorption Coefficient	-0.348	0.161	0.191
Insulation Emissivity	0.033	0.113	0.115

When only the simulations in which flame spread occurred were considered, the duration of the simulation was most sensitive to the heat of combustion, the wood and insulation absorption coefficients, the wood thermo-physical properties, wood surface thickness definition, and the kinetics of wood pyrolysis.

It is evident from a comparison of Table 9 and Table 10 that the input parameters that generally facilitate flame spread necessarily also decrease the duration of the simulation because flames are allowed to spread to the ventilator more quickly. This observation leads to the conclusion that a balance must be struck between the most important parameters to calibrate the model against physical observations. This balance means that the set of parameters that includes the lowest heat of combustion and highest heat of reaction and activation energy while still allowing for ignition of the wood trusses and flame spread will provide the timeline of fire spread, and the wood material properties values can be decreased to increase the amount of time required for flames to reach the ventilator. The properties presented as set #42 in

Table 8 were defined as the set that most closely matched the calibration condition and were used as baseline from which to start the high-resolution simulations.

### 6.3. High-Resolution Simulations

The parameters defined in set #42 from Table 8 were used as an initial point from which to compare simulation results in simulations of the full-size high-resolution attic space model. The maximum HRRPUA was defined as 1995 kW/m<sup>2</sup>, identical to how it was measured in the model to determine the fire exposure to the attic from the fires on the 6<sup>th</sup> and 7<sup>th</sup> floors. Several modifications were made to the set of parameters after the first simulation to attempt to shift the rate of flame spread to agree more closely with the observations. The final set of parameters that yielded the results closest to reality are provided in Table 11. In an attempt to make the wood trusses less flammable and the rate of flame spread slower and more closely in agreement with the observations at the scene, the char yield was increased to its upper limit that still facilitated ignition of the trusses with the source fire defined as the exposure fire from the 7<sup>th</sup> floor.

**Table 11. Final set of parameters to describe construction elements in attic**

					Wood										Insulation				
SOOT YIELD (g/g)	CO YIELD (g/g)	BURN AWAY	Char Yield (g/g)	Char Density (kg/m <sup>3</sup> )	Thermal Conductivity (W/m <sup>2</sup> K)	Specific Heat (kJ/kgK)	Density (kg/m <sup>3</sup> )	Heat of Reaction (kJ/kg)	Heat of Combustion (kJ/kg)	Absorption Coefficient (1/m <sup>2</sup> )	Emissivity	Arrhenius Pre-Exponential Factor (1/s)	Activation Energy (J/mol)	Wood Stud Thickness (m)	Thermal Conductivity (W/m <sup>2</sup> K)	Specific Heat (kJ/kgK)	Density (kg/m <sup>3</sup> )	Absorption Coefficient (1/m <sup>2</sup> )	Emissivity
0.015	0.004	FALSE	0.6	154	0.09	1.62	640	2400	16400	50000	0.85	3.57E+05	6.75E+04	0.0381	0.08	1.2	36	50000	0.95

#### 6.3.1. Baseline Model

The total HRR from the baseline high-resolution model is provided in Figure 33. The source fire that represented the exposure from the 6<sup>th</sup> and 7<sup>th</sup> floor to the attic space through the open access hatch had a duration of approximately 180 s and is represented in Figure 33 as the local maximum in the time range from 0 to 180 s. The HRR increases steadily to approximately 800 kW after the duration of the source fire, where the total HRR is relatively constant until approximately 3600 s. This pattern is repeated several times with a monotonically increasing total HRR that totals 2 MW by 9000 s. Much of the observed volumetric HRR was localized to the areas in close proximity to the passive vents in that attic roof.

The results of the baseline simulation did not directly agree with the limited available data of the actual fire event. In the fire event, it appeared that there was significant local burning with flames attached to the trusses throughout much of the duration of the fire. These observations were based on video that was captured by firefighters at street level and performing suppression activities in the building during the event. In an attempt to make the results of the simulation more closely resemble these observations, the char yield was increased to 0.6 to effectively decrease the yield of combustible gaseous pyrolyzate, which had the effect of decreasing the equivalence ratio and slowed the spread of the interface between the under-ventilated area and the oxygen-rich area. This increase in the char yield was justified because the structural truss elements were forced to conform with the underlying mesh, which increased the total surface area beyond the actual surface area of the trusses. A higher char yield assigned to the truss element surfaces decreased the total flammable gaseous pyrolyzate production rate to more closely agree with the rate expected from the actual trusses that had less exposed surface area.

With the increased char yield, the first indication of intermittent flames at the southeasternmost ventilator that was located on the roof above the fire room was approximately 700 s. Plots of the HRRPUV isosurface (>50 kW/m<sup>3</sup>) at 700 s are shown in Figure 34 where flames are identified with the color blue. It is evident in the figure that localized flaming in the attic appears directly above the open access hatch as well as some intermittent flames at the ventilator slightly east of the fire rooms.

The same view of the modeled geometry with plots of HRRPUV isosurface at 9000 s is shown in Figure 35 with fire again colored blue. In the figure, it is evident that there is a moving flame front ranging from the bottom center to the upper right of the image and moving toward unburned trusses on the left side of the image. It is evident that localized flames are present at all ventilators within the flaming region at this time.

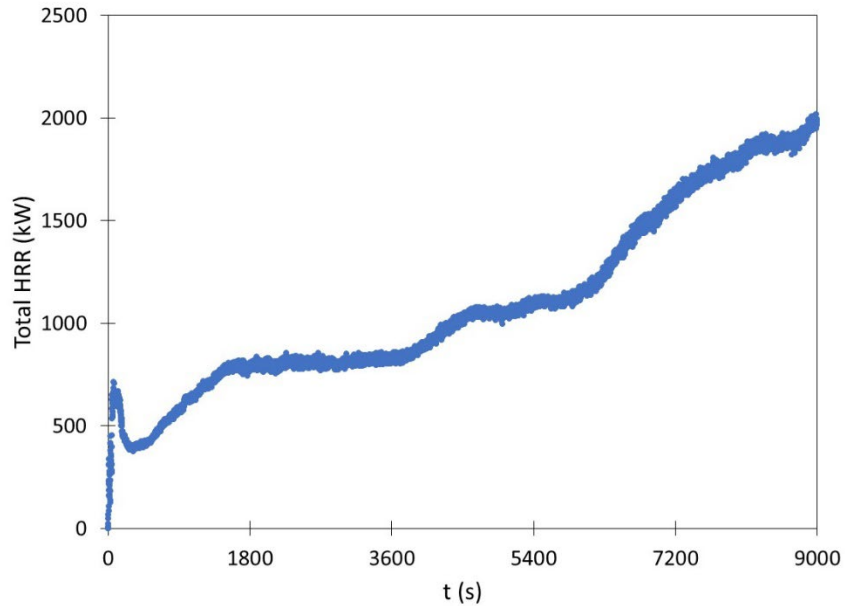


**Figure 33. Total HRR in Baseline High-Resolution Model Simulation**

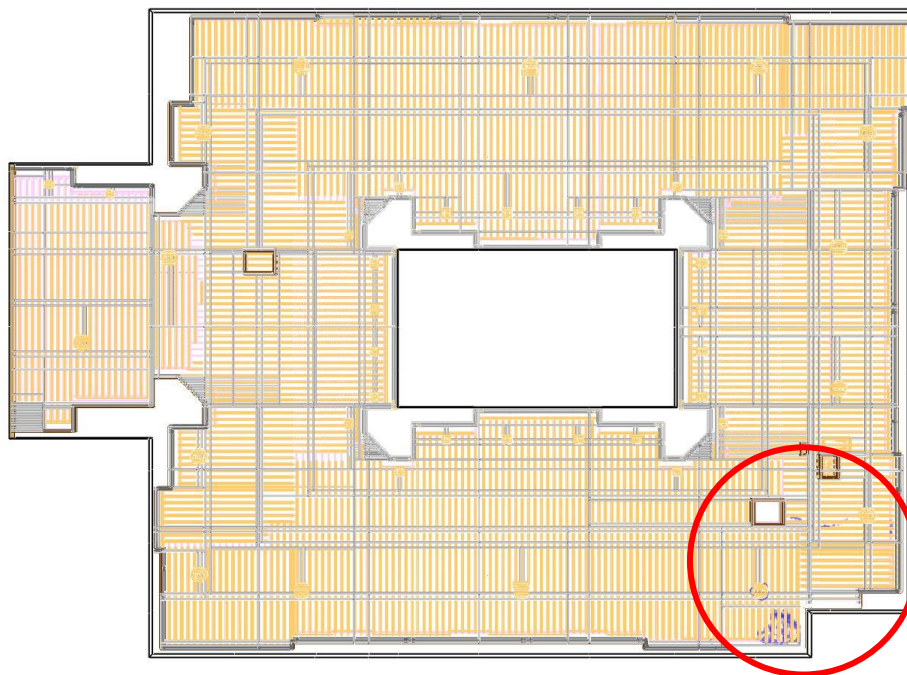


**Figure 34. HRRPUV isosurfaces (colored blue) showing locations of burning at t=700 s**

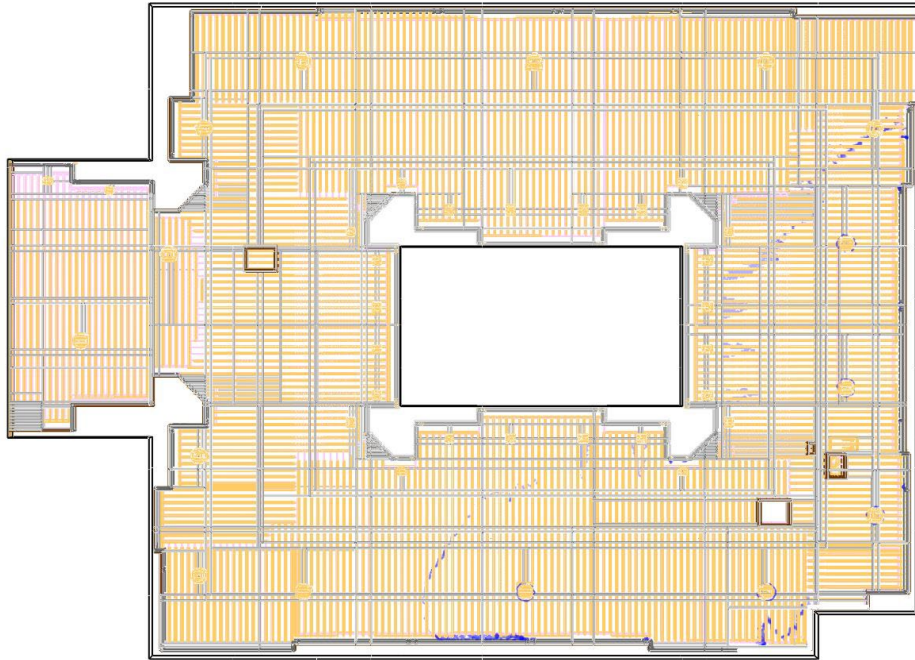


**Figure 35. HRRPUV isosurfaces (colored blue) showing locations of burning at t=9000 s**

The observation that was the most significant contributor to calibration of the model was the observation of flames at the roof level approximately 30 minutes after flames were observed through the ceiling of the 7<sup>th</sup> floor apartment. The set of properties that provide the best agreement with this major observation yields a prediction of flames at the roof ventilator at approximately 700 s (~12 minutes after flames enter the attic). This discrepancy may be attributed to the combustion model invoked in FDS that did not account for smoldering solid-phase combustion. The discrepancy may also be attributed to an erroneous interpretation of the observation of flames at the roof where flame was actually present at the ventilator long before it was visible from the street level. Other phenomena that were observed in some of the video from the incident were not represented in the model and may form the basis for future research.

Because of the relative lack of information about the evolution of the flames beyond the videos focused on the flame spread from the 6<sup>th</sup> floor to the 7<sup>th</sup> floor, it is difficult to identify the phenomena that are not adequately included in the models to which the flame spread is sensitive. The features that were not included in the model that may have contributed to deviations between the observations and the simulation results were the ability for fire to burn through the attic roof and the façade assemblies at the exterior faces of the attic, roof collapse, decrease of thickness and degradation of the properties of the attic insulation, active ventilation by firefighters from the seventh floor and the fire-rated wall, active suppression from the seventh floor and the fire-rated wall, and the effects of wind.

### 6.3.2. Baseline Model with Sprinklers

The total HRR from the baseline high-resolution model as well as from the high-resolution model with sprinklers activated is provided in Figure 36. Figure 36 shows a significantly lower total HRR throughout the duration of the simulation. It is evident that the simulation with the active sprinklers goes through periods of fire growth and suppression as additional sprinklers are activated. The persistence of the fire is most likely attributed to the relatively complicated geometry of the trusses that may shield some of the burning surfaces from delivery of water droplets. The expectation for this simulation was for the sprinklers to suppress and eventually extinguish the fire as it burned through the attic and limit the extent to which the fire spread. The simulated sprinklers appear to be consistent with this expectation in that only limited spread of the fire is allowed. Additional research is recommended to determine the precise reason the sprinklers did not completely extinguish the fire.

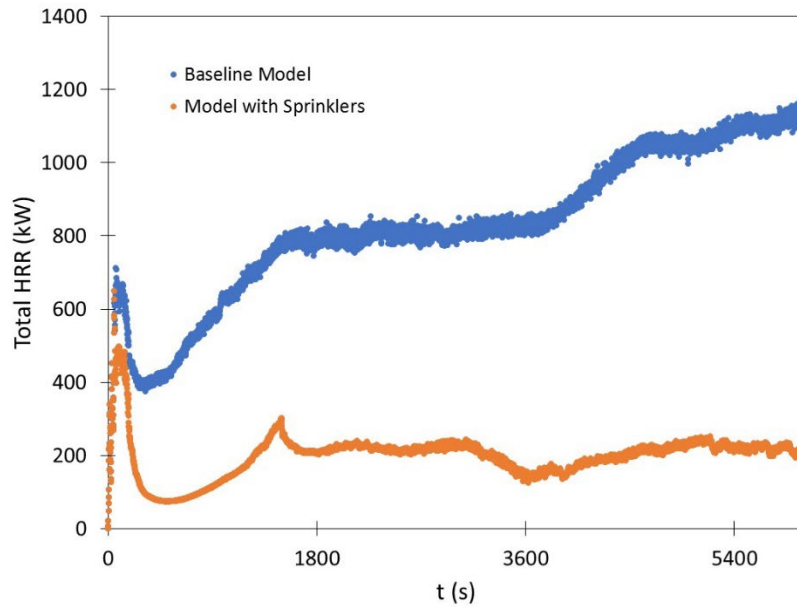


**Figure 36. Total HRR from High-Resolution Model with Sprinklers Active**

6.3.3. Baseline Model with 3,000 sq. ft. Area Partitioned

The total HRR from the baseline high-resolution model as well as from the high-resolution model with a 3,000 sq. ft. area partitioned is provided in Figure 37. Figure 37 shows a significantly lower total HRR throughout the duration of the simulation for the modified geometry compared to the baseline case. Figure 38 shows the extent of flame spread in the attic in this simulation. The relatively steady, lower total HRR is likely attributed to a ventilation limitation because the partitions were modeled to prevent the flow of all air and fuel. The image in Figure 38 is consistent with this hypothesis because there is local flaming in the vicinity of the three rooftop ventilators within the partitioned area.

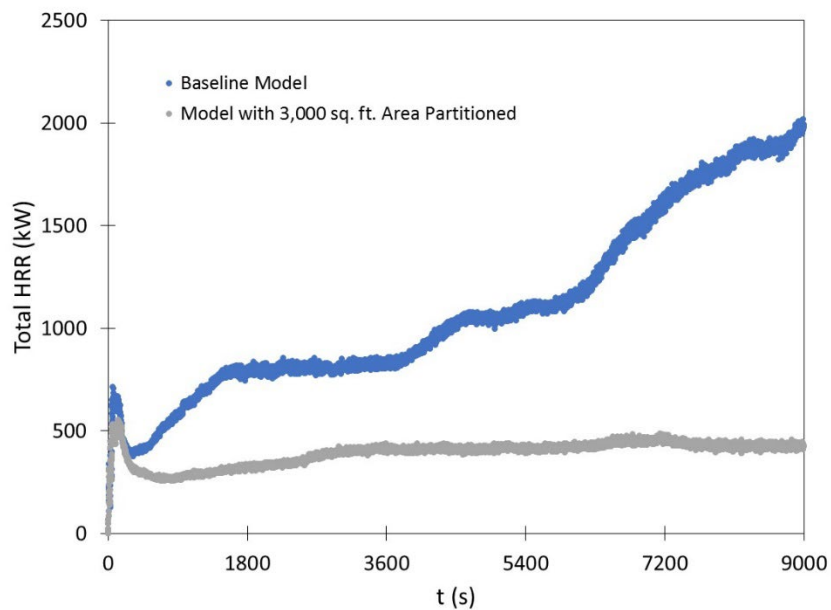


**Figure 37. Total HRR from High-Resolution Model with 3,000 sq. ft. Area Partitioned**

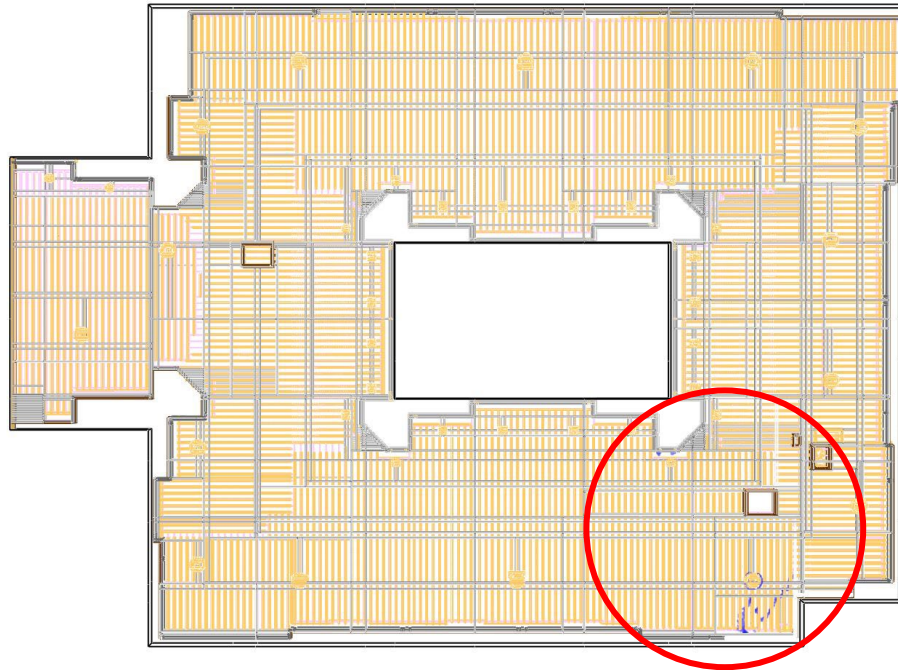


**Figure 38. HRRPUV isosurfaces (colored blue) showing locations of burning at t=9000 s**

6.3.4. Baseline Model with 10,000 sq. ft. Area Partitioned

The total HRR from the baseline high-resolution model as well as from the high-resolution model with a 10,000 sq. ft. area partitioned is provided in Figure 39. Figure 39 shows the total HRR that deviates from the baseline total HRR at approximately 4500 s and remains relatively steady at approximately 1 MW while the baseline HRR continues to increase.

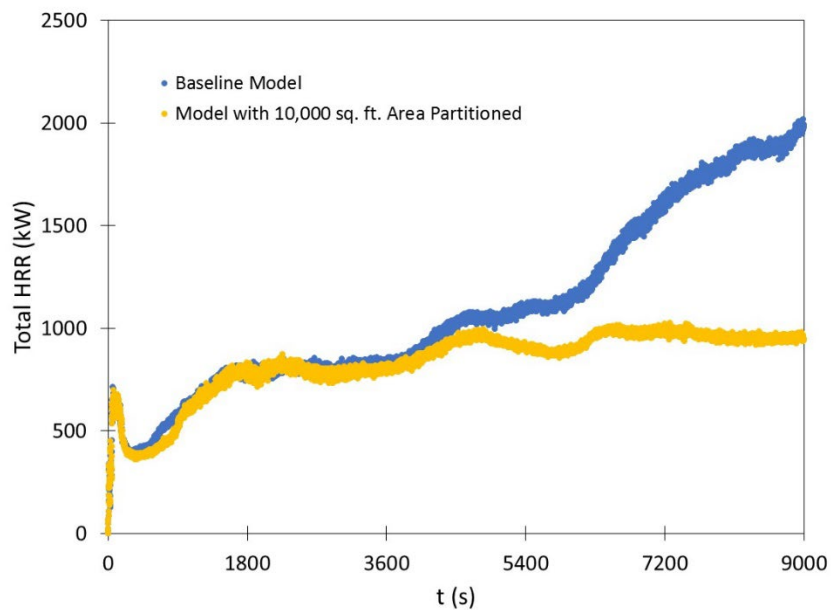


**Figure 39. Total HRR from High-Resolution Model with 3,000 sq. ft. Area Partitioned**

Figure 40 shows an image of the extent of flame spread at 9000 s. The flames generally appear to be localized in the vicinity of the passive ventilators at the roof of the building. This observation is consistent with ventilation in the attic being the limiting factor for flame spread and explains why the total HRR for the simulation with the larger partitioned area that contains more ventilators is higher than that for the simulation with the smaller partitioned area.

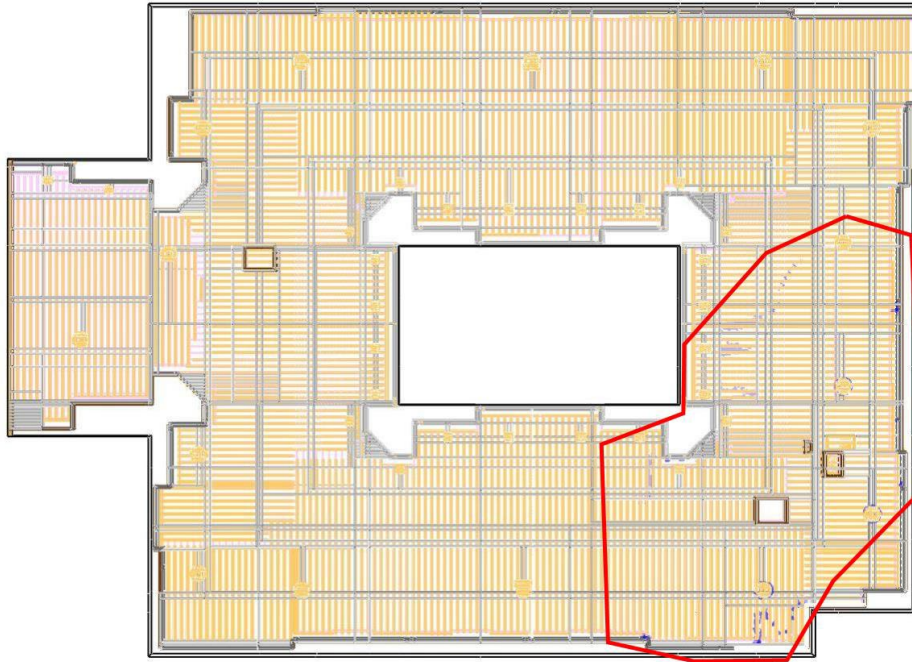


**Figure 40. HRRPUV isosurfaces (colored blue) showing locations of burning at t=9000 s**

## 6.4. Low-Resolution Simulations

### 6.4.1. Baseline Simulation

The total HRR for the simulation of the baseline low-resolution model is provided in Figure 41. The maximum HRR of approximately 212 MW occurs at approximately 1400 s. In the figure, the 8.4 MW source fire persisted at that HRR for a relatively short period of time before significant growth was evident. Initial growth of the fire involved flames spreading up the exposed wood studs in the original fire room to the structural floor trusses and the combustible sheathing defined as the underside of the flooring assembly and radial spread outward to other rooms on that floor. Figure 42 shows the extent of flame spread at 1400 s when the HRR was at its maximum value emphasized by the red line drawn on the figure. At 1400 s, much of the available fuel in the original fire room was burned out, leaving no combustible mass available. The same phenomenon happened after 1400 s when the HRR dropped precipitously toward 0. It is evident that although large portions of the fire were extinguished at the end of the simulation, there was still a sizeable HRR of approximately 12 MW sustained by available unburned wood construction.

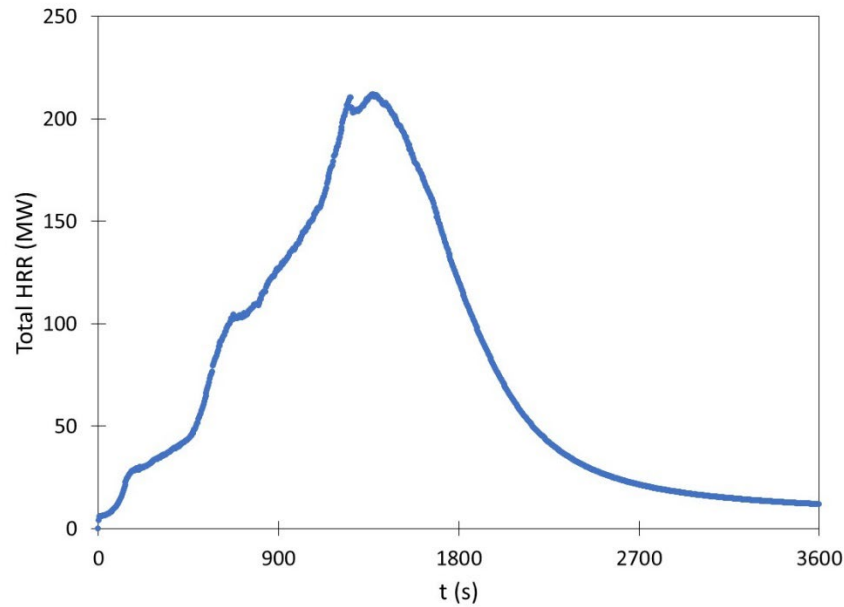


**Figure 41. Baseline Low-Resolution Model Simulation Total HRR**



**Figure 42. Baseline Low-Resolution Model Simulation at Time of Maximum HRR (t=1400s)**

#### 6.4.2. Baseline Model with 10,000 sq. ft. Area Partitioned

The total HRR for the simulation of the baseline low-resolution model with gypsum board installed to create a 10,000 sq. ft. partition is provided in Figure 43. The maximum HRR of approximately 102 MW occurs at approximately 770 s. The HRR evolution appears to closely track that of the baseline model simulation up to the approximate maximum HRR, which corresponds to the time that the flame spreads to the partition on the south and east sides of the building. Figure 44 shows the extent of flame spread at 770 s when the HRR is at its maximum value emphasized by the red line drawn on the figure. At 770 s, the flame fronts had reached the partitions and flames migrated toward the window openings. After a relatively steady HRR at approximately 100 MW, the total HRR dropped as available fuel was exhausted and the partitioned area transitioned to fuel-limited burning. It is clear from Figure 43 that installing

gypsum board strategically throughout the building may be an effective method to contain a fire in a wood-constructed building and limit total HRR.

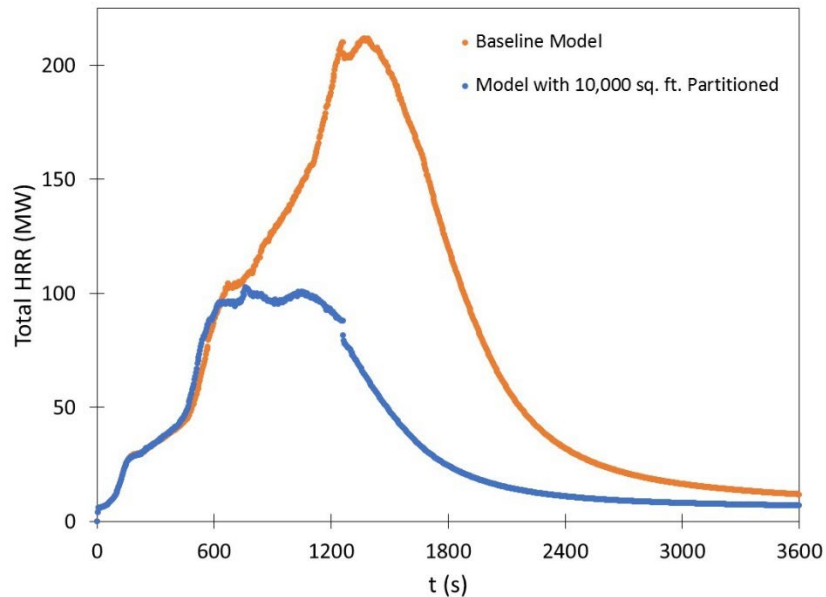


**Figure 43. Baseline Simulation with 10,000 sq. ft. Area Partitioned**

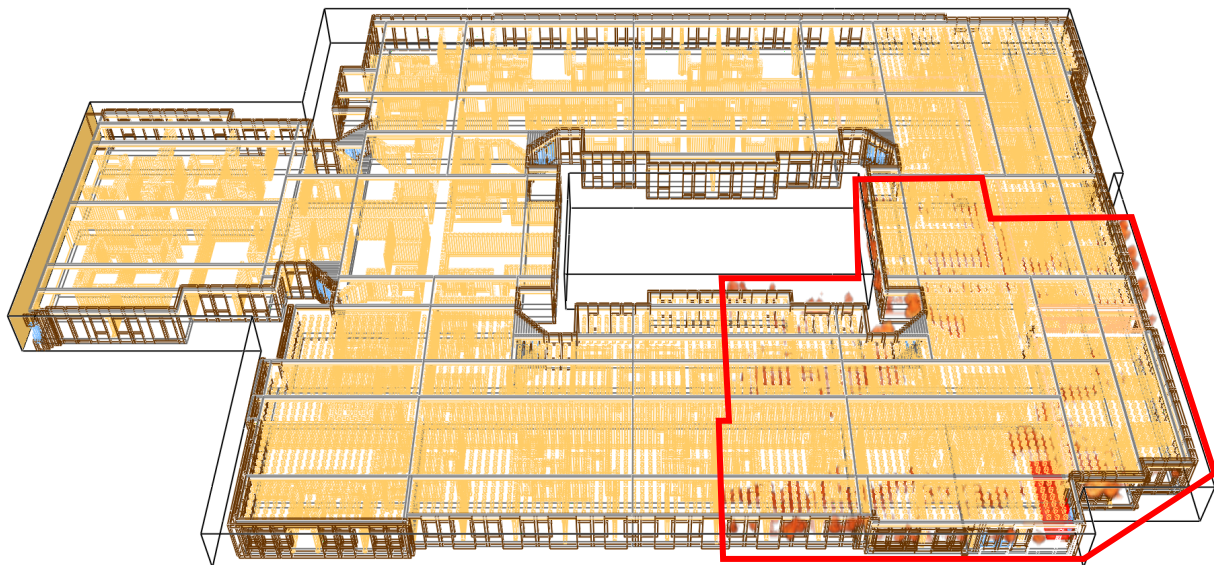


**Figure 44. Low-Resolution Model With 10,000 sq. ft. Area Partitioned Simulation at Time of Maximum HRR (t=770s)**

#### 6.4.3. Baseline Model with Sprinklers Active

The total HRR for the simulation of the baseline low-resolution model with sprinklers active is provided in Figure 45. The simulation progress halted after 781 s because of an apparent divergence. Although the exact reason for the divergence was unclear, this result was replicated multiple times with a modified mesh. The maximum HRR of approximately 18.7 MW occurred at approximately 130 s and the HRR remained steady at approximately 18.7 MW until the simulation halted. The HRR evolution appears to

closely track that of the baseline model simulation up to the approximate maximum HRR, which corresponds to the time at which the first sprinkler was activated. Figure 46 shows the extent of burning at 770 s to provide a direct comparison with the extend of flame spread with the partitions installed. Figure 46 shows that the fire is contained generally to the original fire room and slightly beyond at the same time the fire had spread to the partitions in the case with partitions installed. Had the simulation completely finished, it is expected that the burning wood would have exhausted all of its pyrolyzate fuel and the fire would have extinguished. This result indicates that active sprinklers are very effective at containing flame spread and limiting total HRR in a free burning scenario.

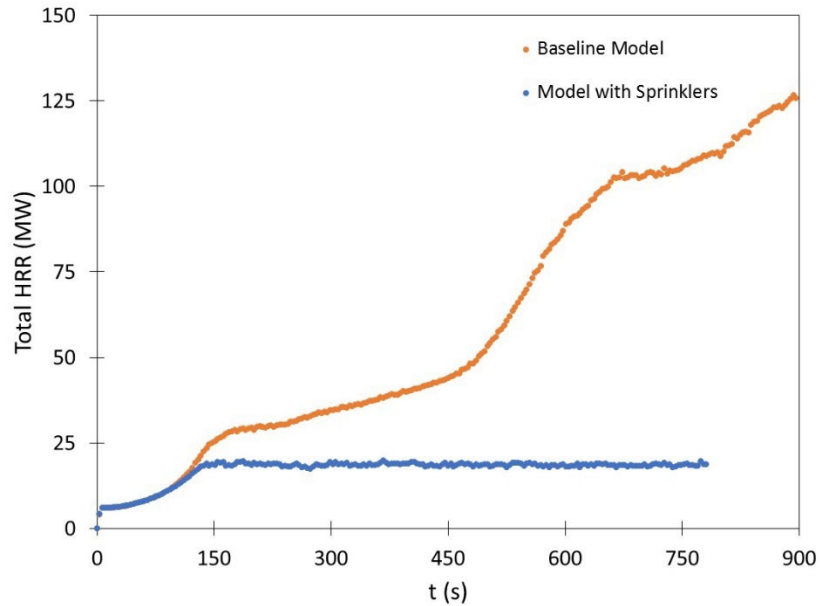


Figure 45. Baseline Simulation with Sprinklers

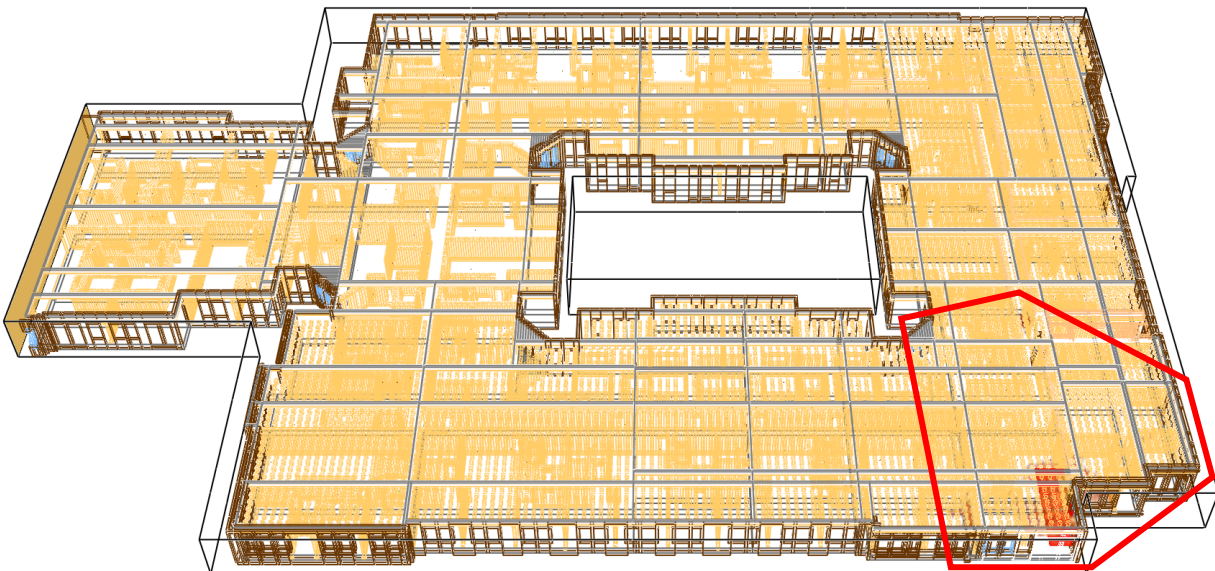


Figure 46. Low-Resolution Model with Sprinklers Simulation at t=770s

#### 6.4.4. Baseline Model with Exterior Walls Removed

The total HRR of the simulations for the baseline model and the baseline model with the exterior walls removed is provided in Figure 47. The maximum total HRR was 47.4 MW and occurred at approximately 500 s. The HRR starts to decrease at 1200 s at the time that the source fire is simulated to burn out and return to a HRR of zero. It is evident that the total HRR is significantly lower when the exterior walls are not installed and finished. With the exterior walls installed, a hot upper gas layer formed and facilitated flame spread, whereas without the walls, there is nothing that forces the hot gases to remain in the building. Additionally, when the fire is ventilation-limited, flames are forced to spread to areas where abundant oxygen is available and unburned fuel is more plentiful. This result indicates that delaying installation and finishing of exterior walls is more effective in reducing fire spread than partitions alone.

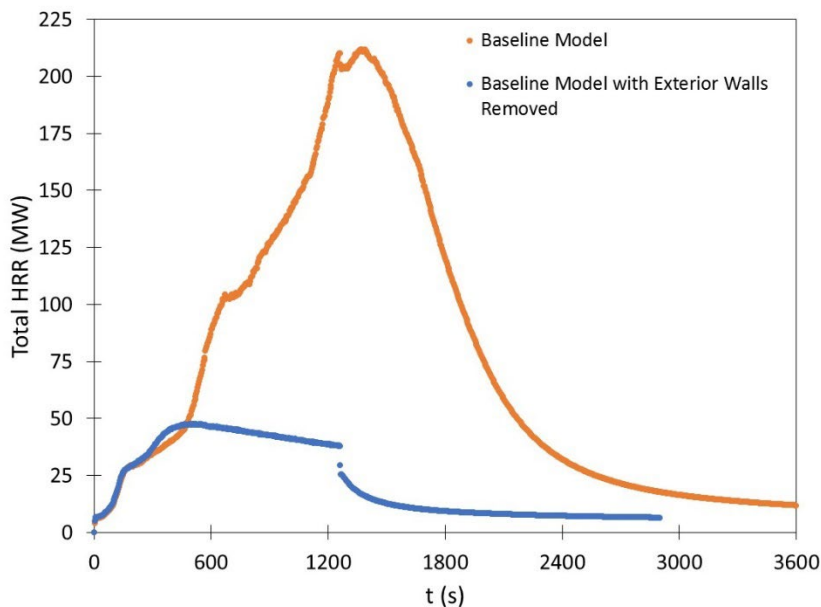


Figure 47. Baseline Simulation with no Exterior Walls

## 7. CONCLUSIONS

An extensive modeling effort was conducted to investigate the effects of various active and passive fire protection strategies in buildings primarily comprised of wood structural elements while those buildings are under construction. This investigation was motivated by a series of high-profile fires in wood-framed construction that were built to code but still suffered catastrophic damage when fires were initiated within the buildings. One particular fire event that this investigation has focused on was the fire at the FUSE 47 building in College Park, MD on April 24, 2017.

This investigation involved modeling of the fire growth in the 6<sup>th</sup> floor, spread to the seventh floor and attic space, and spread through the attic space, using a fine-resolution mesh. The flame spread modeling was compared to observations made at the scene on the day of the incident and in several site visits thereafter. This investigation also involved a set of Monte Carlo simulations to determine the sensitivity of the flame spread modeling results to each of the material properties and degradation reaction parameters for the wood products that acted as fuel in the attic space. Finally, a set of low-resolution models that incorporated other floors that were not involved in the FUSE 47 fire were modeled to determine the overall effect of sprinklers, temporary fire-resistant barriers installed to partition areas of the building, and various levels of completeness of construction on the flame spread and total fire growth.

A set of parameters were determined through the Monte Carlo simulations that provided the best agreement between the high-resolution FDS model and observations of the actual fire event. The best agreement between the simulations and the observations showed a large discrepancy, which was most

likely attributed to the general lack of information about the evolution of the fire during the event, as well as active firefighting measures whose physical phenomena were not incorporated into the model. The incorporation of sprinklers into the high-resolution model of flame spread in the attic decreased the overall HRR, but more research is required before the full effect of sprinklers on flame spread in attic can be determined. Introduction of partitions in the attic space had a profound effect on the total HRR and rate of fire spread in the attic. It appeared evident that by introducing partitions, ventilation was limited to the passive ventilators within the partitioned area, which significantly decreased the total HRR relative to the baseline case.

A baseline low-resolution model was constructed to describe flame spread through a typical floor in the FUSE 47 apartment building when the exterior walls were installed and finished, windows were not installed, and none of the walls or ceilings were installed. Modifications to the baseline case included installation of sprinklers, a gypsum board partition to partition off 10,000 sq. ft. around the source fire, and a case where the exterior walls were not installed, and in place of the walls were exposed wood framing studs. The final results showed that partitions may contain spread of the fire and limit the total overall HRR, removal of exterior walls may be more effective than installation of partitions alone, and sprinklers can be very effective at containing flame spread and may be the most effective fire protection measure investigated.

## 8. REFERENCES

- [1] Weather Underground. Weather Underground - College Park, MD April 24, 2017 <<https://www.wunderground.com/history/daily/us/md/college-park/KCGS/date/2017-4-24.>>
- [2] Hurley MJ, Gottuk D, Hall JR, et al. (eds). *SFPE Handbook of Fire Protection Engineering*. 5th ed. Bethesda, Md, 2016.
- [3] Tenwolde A, McNatt JD, Krahn L. *Thermal Properties of Wood and Wood Panel Products for Use in Buildings*. Oak Ridge, TN, 1988.
- [4] Simpson W, Tenwolde A. Physical Properties and Moisture Relations of Wood. In: *Wood handbook: wood as an engineering material*. Madison, WI, 1999, p. 3.1-3.24.
- [5] Mealy C, Boehmer H, Scheffey J, et al. *Characterization of the Flammability and Thermal Decomposition Properties of Aircraft Skin Composite Materials and Combustible Surrogates*. Atlantic City International Airport, NJ, 2014.
- [6] MacLean JD. Thermal Conductivity of Wood. *ASHVE J* 1941; 13: 380–391.
- [7] Lautenberger C, Fernandez-Pello C. A model for the oxidative pyrolysis of wood. *Combust Flame* 2009; 156: 1503–1513.
- [8] Igaz R, Kristak L, Ruziak I, et al. Thermophysical Properties of OSB Boards versus Equilibrium Moisture Content. *BioResources* 2017; 12: 8106–8118.
- [9] Czajkowski Ł, Olek W, Weres J, et al. Thermal properties of wood-based panels : thermal conductivity identification with inverse modeling. *Eur J Wood Wood Prod* 2016; 74: 577–584.
- [10] Czajkowski Ł, Olek W. Thermal properties of wood-based panels : specific heat determination. *Wood Sci Technol* 2016; 50: 537–545.
- [11] Bellais M. *Modelling of the pyrolysis of large wood particles*. KTH - Royal Institute of Technology, 2007.
- [12] Blasi C Di, Branca C. Kinetics of Primary Product Formation from Wood Pyrolysis Kinetics of Primary Product Formation from Wood Pyrolysis. *Ind Eng Chem Res* 2001; 40: 5547–5556.
- [13] Słopiecka K, Bartocci P, Fantozzi F. Thermogravimetric analysis and Kinetic study of poplar wood pyrolysis. In: *Third International Conference on Applied Energy*. 2011, pp. 1687–1698.
- [14] White RH, DiTenberger MA. Wood Products : Thermal Degradation and Fire. 2001; 9712–9716.
- [15] Branca C, Blasi C Di. Kinetics of the isothermal degradation of wood in the temperature range 528 – 708 K. *J Anal Appl Pyrolysis* 2003; 67: 207–219.
- [16] Bryden KM, Ragland KW, Rutland CJ. Modeling thermally thick pyrolysis of wood. *Biomass and Bioenergy* 2002; 22: 41–53.
- [17] Park WC, Atreya A, Baum HR. Experimental and theoretical investigation of heat and mass transfer processes during wood pyrolysis. *Combust Flame* 2010; 157: 481–494.
- [18] Benichou N, Sultan MA, MacCallum C, et al. *Thermal Properties of Wood , Gypsum and Insulation at Elevated Temperatures*. 2001.
- [19] Hald A. *Statistical Theory with Engineering Applications*. Wiley, 1952.

- [20] Notarianni K. *The Role of Uncertainty in Improving Fire Protection Regulation*. Carnegie Mellon University, 2000.

**APPENDIX A: FDS Input Files Delivered to NIST**

Scenario	FDS file delivered
High-Resolution Baseline	FUSE47_Attic_64.fds FUSE47_Attic_BL (CHID)
High-Resolution Baseline with Sprinklers	FUSE47_Attic_64.fds FUSE47_Attic_MOD1 (CHID)
<i>High-Resolution Baseline with 3,000 sq. ft. Partitioned Area</i>	FUSE47_Attic_64.fds FUSE47_Attic_MOD2_NS (CHID)
<i>High-Resolution Baseline with 10,000 sq. ft. Partitioned Area</i>	FUSE47_Attic_64.fds FUSE47_Attic_MOD3_NS (CHID)
Low-Resolution Baseline	FUSE47_Phase3_181106_mod.fds FUSE47_Phase3_181116 (CHID)
Low-Resolution Baseline with Sprinklers	FUSE47_Phase3_181116_MOD3.fds FUSE47_Phase3_181116_mod3 (CHID)
Low-Resolution Baseline with 10,000 sq. ft. Partitioned Area	FUSE47_Phase3_181116_mod.fds FUSE47_Phase3_181116_mod (CHID)
Low-Resolution Baseline without Exterior Walls	Coarse_MOD-1.fds Coarse_MOD-1 (CHID)